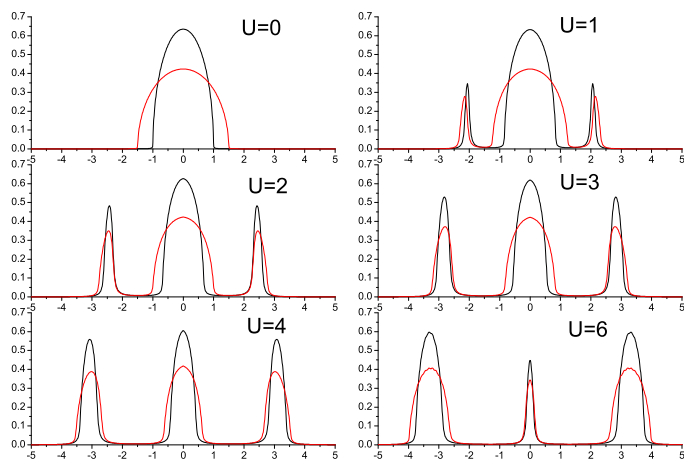
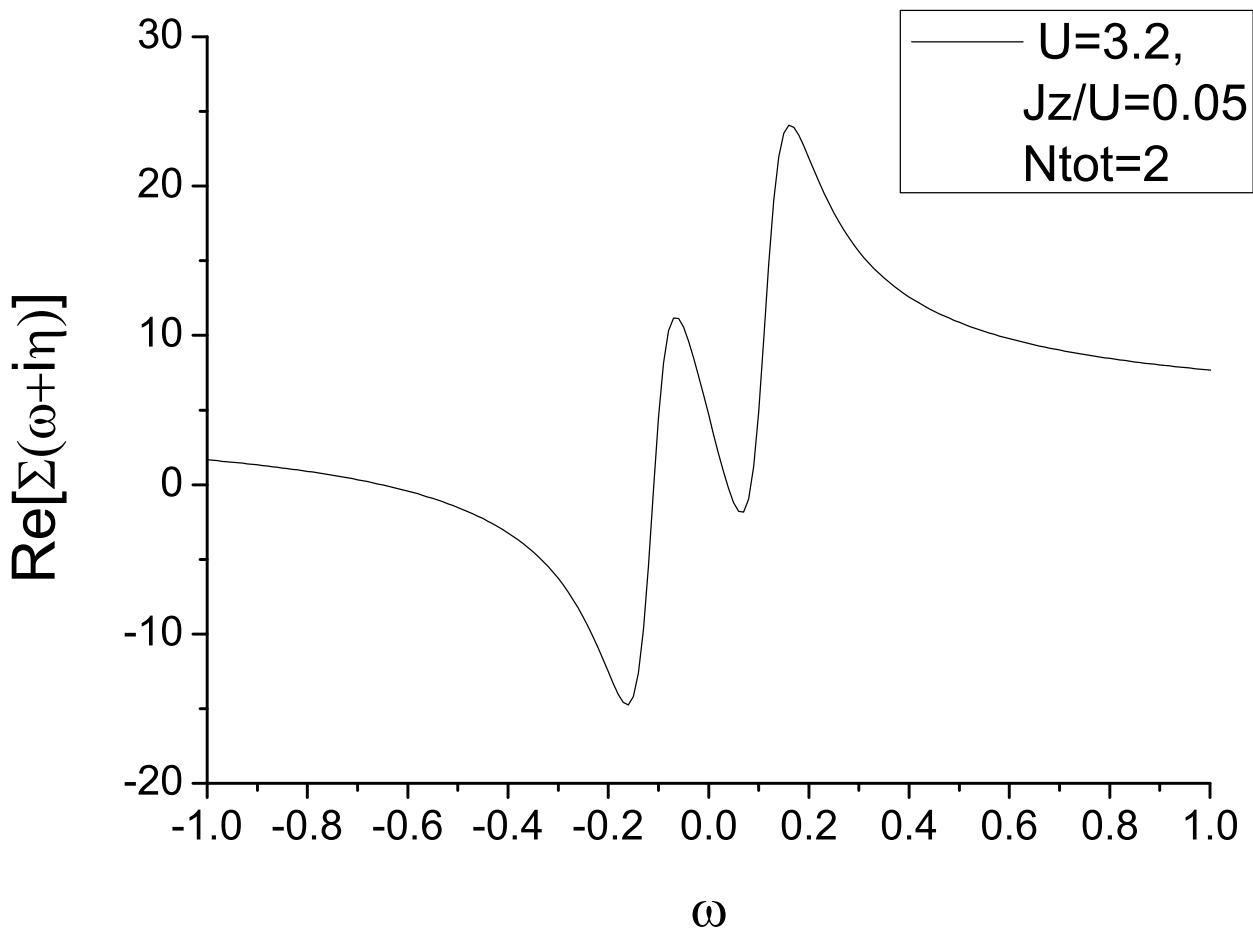
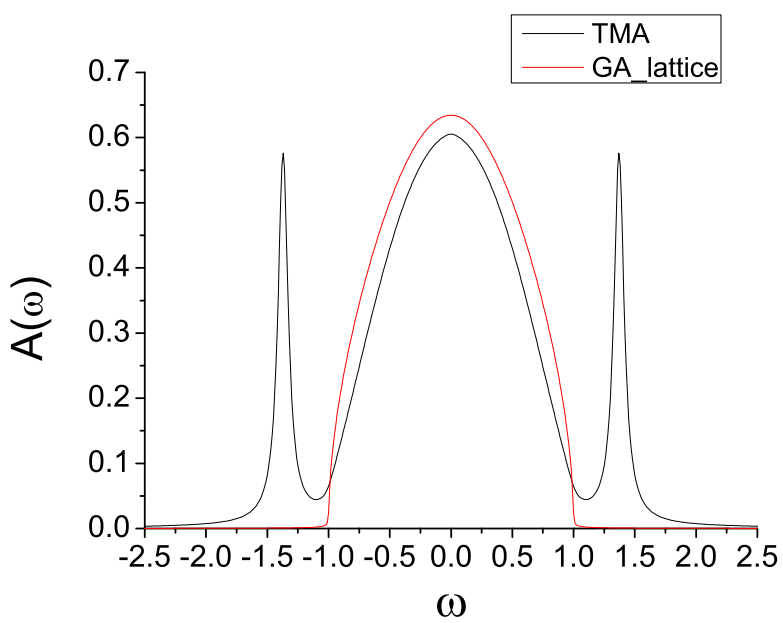


—  $D_1=2t_1=1$   
—  $D_2=2t_2=1.5$









# A Fast Impurity Solver Based on Gutzwiller variational approach

Jia-Ning Zhuang, Lei Wang, Zhong Fang, Xi Dai

(Dated: November 6, 2018)

## Abstract

A fast impurity solver for the dynamical mean field theory(DMFT) named Two Mode Approximation (TMA) is proposed based on the Gutzwiller variational approach, which captures the main features of both the coherent and incoherent motion of the electrons. The new solver works with real frequency at zero temperature and it provides directly the spectral function of the electrons. It can be easily generalized to multi-orbital impurity problems with general on-site interactions, which makes it very useful in LDA+DMFT. Benchmarks on one and two band Hubbard models are presented, and the results agree well with those of Exact Diagonalization (ED).

PACS numbers:

## I. INTRODUCTION

The accurate calculation of the electronic structure of materials starting from first principles is a challenging problem in condensed matter science. The local density approximation (LDA) based on density functional theory (DFT) is a widely used *ab initio* method [1], which has been successfully applied to study the properties of simple metals and semiconductors as well as the band insulators. However, it can not be applied to those materials containing partially filled narrow bands from  $d$  or  $f$  shells, because of the so called strong correlation effect.

In LDA the wave like nature rather than the atomic feature of the electronic state is emphasized, so it is more suitable to describe those wide energy bands contributed by the electrons from outer shells. While for the electrons from those unclosed inner shells like  $3d$  or  $5f$  shells, some atomic features such as the multiplet structure remain, which are poorly described by LDA. Therefore for those strongly correlated materials, we have to implement LDA with some many-body techniques which can deal with the strong correlation effect and capture most of the atomic features.

One notable example of the first-principle schemes is the LDA+U method [2], which can successfully describe many interesting effects such as spin, orbital and charge ordering in transition metal compounds [3]. Although LDA+U can capture the static orbital and spin dependent physics quite well, it still can not consider the dynamical correlation effect, which causes lots of interesting phenomena like Mott transition [4] [5] [6].

Another attempt is to use Gutzwiller variational approach [7] [8] to take into account the correlation effect (LDA+G), which is superior to LDA+U and has been successfully applied to many systems [9] [10] [11]. LDA+G treatment has its advantage in describing ground state and low energy excited states, but it can not properly describe the finite temperature and dynamical properties due to the lack of high energy excited states. In order to capture the overall features of a correlated materials, more sophisticated approaches are needed.

During the past twenty years, the dynamical mean field theory (DMFT) [12] has been quickly developed to be a powerful method to solve the strongly correlated models on the lattice. DMFT maps the lattice models to the corresponding quantum impurity models subject to self-consistency conditions. Unlike the normal static mean field approaches, DMFT keeps the full local dynamics induced by the local interaction. DMFT has been successfully

applied to various of correlation problems, such as the Mott transition in Hubbard model [13] [14], the pseudo gap behavior in high  $T_c$  cuprates [15] and the heavy fermion system [16] [17]. Since DMFT can capture quite accurately the correlation feature induced by the on-site Coulomb interaction and LDA can take care of the periodic potential as well as the long range part of the Coulomb interaction, the combination of the two methods should be a very useful scheme for the first principle calculation of correlation materials. In the past twenty years, LDA+DMFT has been developed very quickly and successfully applied to many systems[18], see [19] [20] [21] and [22] for reviews of the recent developments and applications.

In LDA+DMFT, one encounters the problem of how to efficiently solve quantum impurity problems with self-consistently determined bath degrees of freedom. A fast impurity solver can be regarded as the *engine* of DMFT, which determines the efficiency and accuracy of DMFT. Many impurity solvers have been developed in the past twenty years, which can be divided into analytical methods and numerical methods. The analytical methods include equation of motion (EOM) method [23], Hubbard-I approximation [24] [25], iterative perturbation theory (IPT) [26] [27], the Non-crossing approximation(NCA) [28] and the fluctuation exchange approximation(FLEX) [29]. And the numerical methods include exact diagonalization (ED) [30], Hirsch-Fye Quantum Monte Carlo methods [31] [32] and the numerical renormalization group (NRG) [33]. Most recently a powerful continuous-time quantum Monte Carlo (CTQMC) solver [34] [35] has also been developed and applied to several realistic materials[36] [37].

All these impurity solvers have their own advantages and the limitations as well. Since most of the novel quantum phenomena in condensed matter physics happen in very low temperature, it is always very important for us to study the low temperature properties of the correlated materials using LDA+DMFT. Up to now, the impurity solvers which can work at extremely low temperature are ED, IPT and NRG. Among them, IPT can only apply to the single band system, ED and NRG are numerically quite heavy for a general multi-band system. Therefore it is very useful to develop an impurity solver working at zero temperature, which satisfies the following criteria. i) It can capture both the low energy quasi-particle physics and the high energy Hubbard bands. ii) It works with real frequency and gives the real time dynamical properties directly. iii) It is easy to be generalized to realistic multi-band systems.

Here we propose a fast impurity solver based on Gutzwiller variational approach[9] which has the above three advantages. Gutzwiller variational wave function associated with Gutzwiller approximation was first proposed to deal with lattice problems such as the Hubbard model and the periodical Anderson model[38] [39]. In the present paper, we apply a generalized Gutzwiller method called Two Mode Approximation (TMA) to calculate the Green's function for a quantum impurity model generated by DMFT. TMA is first proposed in reference[40] to calculate the spectral function for the lattice mode. Here we generalize it to the quantum impurity problem and make it a useful impurity solver for DMFT.

In TMA three different types of variational wave functions are constructed for the ground states, low energy quasi-particle states and high energy excited state respectively. All the variational parameters appearing in different wave functions are determined by minimizing the ground state energy, based on which we can obtain the electronic spectral functions over the full frequency range. The computational time is mainly determined by the minimization of the ground state energy and is similar with the previous study on lattice problem[41], which can be easily done even on a single PC. This makes the present approach a fast general solver for LDA+DMFT studies.

The paper is organized as follows. In section II we give the derivation of the method and prove that the sum rule for the electronic spectral function is satisfied. In Section III we benchmark our new impurity solver on the two-band Hubbard model with DMFT+ED. Finally a summary and the conclusions are made in section IV.

## II. DERIVATION OF THE METHOD

### A. Gutzwiller ground state

Let us first consider the following multi-orbital impurity Hamiltonian

$$\begin{aligned}
\hat{H}_{imp} &= \hat{H}_{band} + \hat{H}_{local} + \hat{H}_V \\
\hat{H}_{band} &= \sum_{k\sigma} \epsilon_{k\sigma} \hat{c}_{k\sigma}^+ \hat{c}_{k\sigma} \\
\hat{H}_{local} &= \sum_{\sigma, \sigma'} U_{\sigma\sigma'} \hat{n}_{f\sigma} \hat{n}_{f\sigma'} + \sum_{\sigma} \varepsilon_{\sigma} \hat{n}_{f\sigma} \\
\hat{H}_V &= \sum_{k\sigma} V_{k\sigma} (\hat{c}_{k\sigma}^+ \hat{f}_{\sigma} + h.c.)
\end{aligned}$$

where  $k$  denotes the energy levels in the bath and  $\sigma$  is the joint index for orbital and spin. In Gutzwiller variational approach, the ground state of the above Hamiltonian can be written as

$$|\Psi\rangle = \hat{P}|0\rangle \quad (1)$$

Where  $\hat{P}$  is the Gutzwiller projector and  $|0\rangle$  is a single Slater Determinant like wave function. Both of  $\hat{P}$  and  $|0\rangle$  will be determined by minimizing the ground state energy. Following reference [9], the Gutzwiller projector can be written in terms of the projection operators of the atomic eigen states as

$$\hat{P} = \sum_{\Gamma} \frac{\sqrt{m_{\Gamma}}}{\sqrt{m_{\Gamma}^0}} \hat{m}_{\Gamma} \quad (2)$$

In equation (2), the operator  $\hat{m}_{\Gamma} \equiv |\Gamma\rangle\langle\Gamma|$  is the projector to the eigen states  $|\Gamma\rangle$  of the atomic Hamiltonian  $\hat{H}_{local}$ , and  $m_{\Gamma}$  are the variational parameters introduced in the Gutzwiller theory. Note that if  $\hat{H}_{local}$  only contains density-density interactions, the atomic eigen states are known as the Fock states as the following[9],

$$\begin{aligned}
\Gamma \in \{ &\emptyset; (1), \dots, (2N); (1, 2), (2, 3), \dots, (2N - 1, 2N) \\
&; \dots, (1, \dots, 2N) \}
\end{aligned} \quad (3)$$

,where  $N$  is the number of orbitals.  $m_{\Gamma}^0$  is defined as

$$m_{\Gamma}^0 \equiv \langle 0 | \hat{m}_{\Gamma} | 0 \rangle \quad (4)$$

Using the operator equalities

$$\hat{m}_\Gamma = \prod_{\sigma \in \Gamma} \hat{n}_{f\sigma} \prod_{\sigma \notin \Gamma} (1 - \hat{n}_{f\sigma}) \quad (5)$$

$$\hat{n}_{f\sigma} = \sum_{\Gamma \ni \sigma} \hat{m}_\Gamma \quad (6)$$

with the definition  $n_{f\sigma}^0 \equiv \langle 0 | \hat{n}_{f\sigma} | 0 \rangle$  and  $n_{f\sigma} \equiv \langle \Psi | \hat{n}_{f\sigma} | \Psi \rangle$ , one can prove that  $m_\Gamma^0 = \prod_{\sigma \in \Gamma} n_{f\sigma}^0 \prod_{\sigma \notin \Gamma} (1 - n_{f\sigma}^0)$ ,  $n_{f\sigma}^0 = \sum_{\Gamma \ni \sigma} m_\Gamma^0$  and  $n_{f\sigma} = \sum_{\Gamma \ni \sigma} m_\Gamma$ . We would emphasize that  $n_{f\sigma}^0 = n_{f\sigma}$  for Gutzwiller type wave functions with pure density-density interaction, which greatly simplify the computation[9, 10]. Therefore the Gutzwiller ground state energy of this impurity model reads

$$E_g = \frac{\langle 0 | \hat{P} \hat{H}_{imp} \hat{P} | 0 \rangle}{\langle 0 | \hat{P}^2 | 0 \rangle} \quad (7)$$

the denominator can be expressed as

$$\langle 0 | \hat{P}^2 | 0 \rangle = \sum_{\Gamma} m_\Gamma = 1$$

while the numerator can be calculated by decomposing the projectors as in equation (5) and applying the Wick's theorem[42]. Finally we obtain the ground state energy as

$$\begin{aligned} E_g &= \sum_{k\sigma} \epsilon_{k\sigma} \langle 0 | \hat{c}_{k\sigma}^+ \hat{c}_{k\sigma} | 0 \rangle + \sum_{\Gamma} E_\Gamma m_\Gamma \\ &+ \sum_{k\sigma} z_\sigma V_{k\sigma} \langle 0 | \hat{c}_{k\sigma}^+ \hat{f}_\sigma + h.c. | 0 \rangle \end{aligned}$$

with

$$z_\sigma = \sum_{\Gamma \ni \sigma, \Gamma' = \Gamma \setminus \sigma} \frac{\sqrt{m_\Gamma m_{\Gamma'}}}{\sqrt{n_{f\sigma}^0 (1 - n_{f\sigma}^0)}}$$

The ground state wave function  $|\Psi\rangle$  can be obtained by minimizing the above energy functional respect to the  $m_\Gamma$  and non-interacting wave function  $|0\rangle$ [9, 10] along with the following constraints.

$$\sum_{\Gamma} m_\Gamma = 1 \quad (8)$$

$$n_{f\sigma} = \sum_{\Gamma \ni \sigma} m_\Gamma \quad (9)$$

## B. zero-temperature Green's function

For the impurity Hamiltonian Eq.(1), the retarded Green's function for the electrons on the impurity site reads

$$G_{\sigma}^{imp}(\omega + i\eta) = \sum_n \frac{\langle \Psi | \hat{f}_{\sigma} | n \rangle \langle n | \hat{f}_{\sigma}^{\dagger} | \Psi \rangle}{\omega + i\eta - E_n + E_g} + \sum_m \frac{\langle \Psi | \hat{f}_{\sigma}^{\dagger} | m \rangle \langle m | \hat{f}_{\sigma} | \Psi \rangle}{\omega + i\eta + E_m - E_g} \quad (10)$$

where  $|\Psi\rangle$  is the ground state of  $\hat{H}_{imp}$  with the eigen energy  $E_g$ ,  $|n\rangle$  ( $|m\rangle$ ) are the eigenstates of  $\hat{H}_{imp}$  with one more (less) electron than the ground state.  $E_n$  and  $E_m$  are the corresponding eigenvalues. The above expression is exact if the summation of  $n$  and  $m$  includes all the eigenstates. In the present paper, we apply the two mode approximation (TMA) to solve the quantum impurity problem, in which we limit the above summation in a truncated Hilbert space formed by finite number of excited states over the Gutzwiller variational ground state [40, 43]. In order to capture the basic feature of the electronic spectral function efficiently, we have to include two types of excited states in TMA, namely the quasi-particle excitations which give the right Fermi liquid behavior in low energy, and the high energy excited states which are responsible for the Hubbard bands or the atomic multiplet features. The former are called quasi-particle states and the latter are called bare-particle states in the present paper[40]. The ansatz for the excited states are the following,

$$\begin{aligned} | + k\sigma \rangle &= \hat{c}_{k\sigma}^{\dagger} \hat{P} | 0 \rangle \\ | UHB \rangle &= \hat{f}_{\sigma}^{\dagger} \hat{P} | 0 \rangle \\ | QE \rangle &= \hat{P} \hat{f}_{\sigma}^{\dagger} | 0 \rangle \\ | - k\sigma \rangle &= \hat{c}_{k\sigma} \hat{P} | 0 \rangle \\ | LHB \rangle &= \hat{f}_{\sigma} \hat{P} | 0 \rangle \\ | QH \rangle &= \hat{P} \hat{f}_{\sigma} | 0 \rangle \end{aligned}$$

where  $|QE\rangle$  ( $|QH\rangle$ ) are the quasi-particle (quasi-hole) states,  $|UHB\rangle$  ( $|LHB\rangle$ ) are the bare-particle (bare-hole) states, and  $| + -k\sigma \rangle$  represent the excitations in the bath.

The excited states listed above are neither orthogonal nor normalized, thus we have to calculate the overlaps  $\mathcal{O}_{\alpha\beta} \equiv \langle \alpha | \beta \rangle$  and the matrix elements of the Hamiltonian  $\mathcal{H}_{\alpha\beta} \equiv$

$\langle \alpha | \hat{H} | \beta \rangle$  in this truncated Hilbert space. This procedure could be easily done by applying Wick's theorem. We list all the necessary matrix elements and overlaps in the Appendix.

In order to evaluate the Green's function using expression (10), we have to first obtain the eigen states and eigen values by solving the following generalized eigen equation in the truncated Hilbert space.

$$\mathcal{H}|l\rangle = E_l \mathcal{O}|l\rangle$$

Therefore  $|l\rangle$  form a complete basis for the truncated Hilbert space and the completeness condition  $\sum_l |l\rangle \langle l| = 1$  is satisfied within the truncated Hilbert space. Since both the states  $\hat{f}_\sigma^\dagger \hat{P}|0\rangle$  and  $\hat{f}_\sigma \hat{P}|0\rangle$  are fully included in the contained Hilbert space, it is easy to prove that

$$\begin{aligned} \left(-\frac{1}{\pi}\right) \text{Im}[G_\sigma^{\text{imp}}(\omega + i\eta)] &= \langle \Psi | \hat{f}_\sigma \hat{f}_\sigma^\dagger + \hat{f}_\sigma^\dagger \hat{f}_\sigma | \Psi \rangle \\ &= 1 \end{aligned}$$

, which is the sum rule of the impurity Green's function.

### III. BENCHMARK

#### A. Impurity Spectral function

First of all we check the spectral function obtained by TMA for a single orbital impurity model with particle-hole symmetry. The density of states for the heat bath is chosen to be the semicircle with the half-width  $D = 1$ . The spectral functions for the electron on the impurity site with different Hubbard interaction  $U$  are shown in Fig.(1).

From Fig.(1) we find that the spectral function contains three parts, the quasi-particle peak and two Hubbard bands. With the increment of  $U$ , the spectral weight transfers from the low energy quasi-particle part to the Hubbard bands. And in large  $U$  limit, the distance between two Hubbard bands approaches  $U$ . All these features are consistent with the previous studies on the symmetric Anderson model [44]. In Fig.(2), we compare one spectral function for an Anderson impurity model obtained by TMA with that by the normal Gutzwiller Approximation (GA)[7, 9] for the lattice model, which only contains the quasi-particle part as



$$G_{imp}^{GWMF}(\omega + i\eta) = \frac{z^2}{\omega + i\eta + \tilde{\mu} - z^2\Delta(\omega + i\eta)} \quad (11)$$

Compared with normal Gutzwiller approximation (GA lattice), it is very clear that TMA can reproduce very nicely the low energy quasi-particle part with slightly smaller spectral weight. Therefore the current solver can be viewed as the normal Gutzwiller approximation implemented with the Hubbard bands in the high energy part of the electronic spectral functions describing the atomic features.

## B. Used as the impurity solver in DMFT

The present impurity solver can be used in the dynamical mean field theory to study the lattice models. In this paper we have studied both the single-band and two-band Hubbard model at paramagnetic phase with arbitrary fillings.

### 1. Single-band Hubbard model

We start with the single band Hubbard model on the Bethe lattice with half band width  $D = 1$ . First we check the half filling case. We show the spectral function with the increment of  $U$  in Fig.(3), from which we see that the height of quasi-particle peak changes little before Mott transition, but the integral of the quasi-particle spectrum reduces as  $U$  increases. This feature is consistent with the previous results obtained by DMFT+IPT[12].

We show the results for the systems away from half filling in Fig.(4).

With the increment of filling factor from  $N_{tot} = 0.2$  to half filling  $N_{tot} = 1.0$ , the spectral weight continuously transfers from the low energy quasi-particle part to the high energy Hubbard bands, which is consistent with the common understanding that the strong correlation effect is less pronounced when the system is doped away from half filling.

In Fig.(5), we quantitatively compare the density of states (DOS) obtained by DMFT+TMA with that by DMFT+ED. We find quite good agreement between them for both the half filling and non-half filling cases. While we also find two disagreements. Compared with the DMFT+ED results, the total spectral weight of the quasi-particle part is over-estimated while the width of the Hubbard bands is under-estimated by DMFT+TMA.

We have also calculated the quasi-particle weight  $z$ , which is a characteristic quantity describing the strength of the correlation effect and is defined as:

$$z_\sigma = \left(1 - \frac{\partial \text{Re}[\Sigma_\sigma(\omega + i\eta)]}{\partial \omega}\right)^{-1} \Big|_{\omega=0} \quad (12)$$

In Fig.(6) we show quasi-particle weight obtained by DMFT+TMA as the function of  $U$  for different filling factors. In the half filling case, the value of  $z$  decreases as the increment of  $U$  until the critical  $U_c$  for the Mott transition. As shown in Fig.(6),  $U_c$  obtained by DMFT+TMA is around 3.6, which is bigger than  $U_{c2} = 2.9$  obtained by DMFT+ED.

In Fig.(7), we compare the  $z$ -factors obtained by DMFT+TMA, Gutzwiller approximation on the lattice model (lattice GA) and DMFT+ED. As discussed in reference[10] and [40], we can only obtain the ground state energy quite accurately by lattice GA, but not for the  $z$ -factor. The reason is quite obvious that in the lattice GA only the low energy quasi-particle states in equation(10) can be considered, which limits the accuracy of  $z$ -factor. While in TMA, we first apply the DMFT scheme to treat the inter-site correlation on a mean field level, which is in principle similar with GA. Then in solving the effective impurity model, we enlarge the variational space by including more excited states, which gives us more accurate description of the low energy excited states and reduces the disagreement in  $z$ -factor with DMFT+ED results as shown in Fig.(7).

## 2. Two-band Hubbard model on the Bethe lattice

The situation becomes more complicated when we consider two-band models. We start with the simplest case that the two bands are degenerate with half bandwidth  $D_1 = D_2 = 1$  and the local part of the Hamiltonian has SU(4) symmetry, which can be written as

$$\hat{H}_{at} = U \sum_b \hat{n}_{b,\uparrow} \hat{n}_{b,\downarrow} + U \sum_{\sigma,\sigma'} \hat{n}_{1,\sigma} \hat{n}_{2,\sigma'} \quad (13)$$

We first show the quasi-particle weight obtained by DMFT+TMA versus  $U$  at different filling factors in Fig(8) and the comparison with DMFT+ED and lattice GA in Fig(9).

The Mott transition at integer fillings can be observed with  $U_c$  slightly larger than the DMFT+ED results. As shown in Fig(9), the improvement of the quasi-particle weight against the lattice GA is quite dramatic, which indicates that even for the low energy quasi-particle part the DMFT+TMA is better than applying the GA directly to the lattice model.

The behavior of  $z$  as the function of the filling factor for fixed  $U = 5.0$  is shown in Fig(10), from which we can find that compared with lattice GA the results obtained by DMFT+TMA is much closer to DMFT+ED.

Next we take the Hund's coupling constant  $J$  into account. Then the atomic Hamiltonian becomes

$$\begin{aligned} \hat{H}_{at} = & U \sum_b \hat{n}_{b,\uparrow} \hat{n}_{b,\downarrow} + U' \sum_{\sigma,\sigma'} \hat{n}_{1,\sigma} \hat{n}_{2,\sigma'} - J \sum_{\sigma} \hat{n}_{1,\sigma} \hat{n}_{2,\sigma} \\ & + J \sum_{\sigma} \hat{c}_{1,\sigma}^+ \hat{c}_{2,-\sigma}^+ \hat{c}_{1,-\sigma} \hat{c}_{2,\sigma} + J(\hat{c}_{1,\uparrow}^+ \hat{c}_{1,\downarrow}^+ \hat{c}_{2,\downarrow} \hat{c}_{2,\uparrow} \\ & + \hat{c}_{2,\uparrow}^+ \hat{c}_{2,\downarrow}^+ \hat{c}_{1,\downarrow} \hat{c}_{1,\uparrow}) \end{aligned} \quad (14)$$

We have the relation  $U - U' = 2J$  for system with cubic symmetry[45]. In the current study, we only keep the longitudinal part of the Hund's rule coupling and neglect the spin flip and pair hopping terms which correspond to the last two terms in the above equation. The results for the full rotational invariance interaction will be studied in detail and published elsewhere.

The quasi-particle weight obtained by DMFT+TMA as the function of  $U$  is shown in Fig.(11). We also compare the results with DMFT+ED in Fig.(12), from which we find that  $U_c$  obtained from TMA is larger than that of DMFT+ED as for the single band model.

In Fig.(11), we find that the Brinkman-Rice(BR) transition is continuous *only* at the point  $J_z = 0$  and first order like for all non-zero  $J_z$ , which is similar with the results in reference [9] obtained by rotational invariant Gutzwiller approximation. This similarity indicates that for degenerate multi-band Hubbard model the basic feature of the BR transition does not strongly relies on the variational invariant treatment of the interaction. Moreover, the similar discontinuity and the tendency that the critical  $U_c$  decreases as  $J_z/U$  increases is also obtained in [46], where the self-energy functional method is used.

However, for the non-degenerate multi-band models, i.e. the two-band model with different band widths, the correct variational invariant treatment is necessary to obtain some of the qualitative features like the orbital selective Mott transition (OSMT)[47]. The detailed study for the OSMT using the variational invariant TMA solver will be presented elsewhere. Here we only give the results for an extreme case, where the band width difference of the two bands is very large. In Fig.(13) and (14), we represent the DOS as well as the quasi-particle weight as the functional of  $U$  with fixed  $J_z/U = 0.3$  and half band width  $D_1 = 1.0$ ,  $D_2 = 6.0$ .

Obviously in such extreme case, the system is in the orbital selective Mott phase which is consistent with reference [48].

#### IV. CONCLUSIONS

In this paper we present a new impurity solver named Two Mode Approximation (TMA) for the multi-orbital quantum impurity model generated by DMFT. By constructing the trial wave functions based on the Gutzwiller variational theory not only for the ground state but also the low energy and high energy excited states, we can obtain the spectral functions of the electrons on the impurity level with the satisfactory of the sum rule. Compared with other popular impurity solvers, TMA works with the real frequency and can obtain both the low energy quasi-particle and high energy Hubbard band behavior. Moreover TMA can be generalized to treat the problem with quite general on-site interaction, which make it a good solver to be used in LDA+DMFT.

ACKNOWLEDGEMENT: The authors would thank Q. M. Liu, X. Y. Deng, Y. Wan and N.H. Tong for their helpful discussions. We acknowledge the supports from NSF of China , and that from the 973 program of China (No.2007CB925000).

#### V. APPENDIX: OVERLAPS AND HAMILTONIAN ELEMENTS

##### A. Overlaps

Define

$$z_\sigma = \sum_{\Gamma \ni \sigma, \Gamma' = \Gamma \setminus \sigma} \frac{\sqrt{m_\Gamma m_{\Gamma'}}}{\sqrt{n_{f\sigma}^0 (1 - n_{f\sigma}^0)}}$$

the non-vanishing overlaps are

$$\langle +k_1\sigma | +k_2\sigma \rangle = \langle 0 | \hat{c}_{k_1\sigma} \hat{c}_{k_2\sigma}^+ | 0 \rangle$$

$$\langle +k\sigma | UHB \rangle = z_\sigma \langle 0 | \hat{c}_{k\sigma} \hat{f}_\sigma^\dagger | 0 \rangle$$

$$\langle +k\sigma | QE \rangle = \langle 0 | \hat{c}_{k\sigma} \hat{f}_\sigma^\dagger | 0 \rangle$$

$$\langle UHB|UHB\rangle = (1 - n_{f\sigma}^0)$$

$$\langle UHB|QE\rangle = z_\sigma(1 - n_{f\sigma}^0)$$

$$\langle QE|QE\rangle = (1 - n_{f\sigma}^0)$$

$$\langle -k_1\sigma | -k_2\sigma\rangle = \langle 0|\hat{c}_{k_1\sigma}^+\hat{c}_{k_2\sigma}|0\rangle$$

$$\langle -k\sigma |LHB\rangle = z_\sigma\langle 0|\hat{c}_{k\sigma}^+\hat{f}_\sigma|0\rangle$$

$$\langle -k\sigma |QH\rangle = \langle 0|\hat{c}_{k\sigma}^+\hat{f}_\sigma|0\rangle$$

$$\langle LHB|LHB\rangle = n_{f\sigma}^0$$

$$\langle LHB|QH\rangle = z_\sigma n_{f\sigma}^0$$

$$\langle LHB|LHB\rangle = n_{f\sigma}^0$$

## B. Hamiltonian Elements

$$\begin{aligned}\hat{H} &= \hat{H}_{band} + \hat{H}_{local} + \hat{H}_V \\ \hat{H}_{band} &= \sum_{k\sigma} \epsilon_{k\sigma} \hat{c}_{k\sigma}^+ \hat{c}_{k\sigma} \\ \hat{H}_{local} &= \sum_{\Gamma} E_{\Gamma} \hat{m}_{\Gamma} + \sum_{\sigma} \varepsilon_{\sigma} \sum_{\Gamma \ni \sigma} \hat{m}_{\Gamma} \\ \hat{H}_V &= \sum_{k\sigma} V_{k\sigma} (\hat{c}_{k\sigma}^+ \hat{f}_{\sigma} + h.c.)\end{aligned}$$

1. *H*-band

Define

$$\begin{aligned}
x_{\sigma\sigma'} &= \sum_{\substack{\Gamma_2 \ni \sigma, \Gamma_2 \ni \sigma' \\ \Gamma_1 = \Gamma_2 \setminus \sigma'}} \frac{\sqrt{m_{\Gamma_1} m_{\Gamma_2}}}{n_{f\sigma}^0 \sqrt{n_{f\sigma'}^0 (1 - n_{f\sigma'}^0)}} \\
y_{\sigma\sigma'} &= \sum_{\substack{\Gamma_1 \ni \sigma, \Gamma_1 \ni \sigma' \\ \Gamma_2 = \Gamma_1 \cup \sigma' \setminus \sigma}} \frac{\sqrt{m_{\Gamma_1} m_{\Gamma_2}}}{\sqrt{n_{f\sigma}^0 (1 - n_{f\sigma}^0) n_{f\sigma'}^0 (1 - n_{f\sigma'}^0)}} \\
w_{\sigma\sigma'} &= \sum_{\substack{\Gamma_2 \ni \sigma, \Gamma_2 \ni \sigma' \\ \Gamma_1 = \Gamma_2 \cup \sigma \cup \sigma'}} \frac{\sqrt{m_{\Gamma_1} m_{\Gamma_2}}}{\sqrt{n_{f\sigma}^0 (1 - n_{f\sigma}^0) n_{f\sigma'}^0 (1 - n_{f\sigma'}^0)}} \\
v_{\sigma\sigma'} &= \sum_{\substack{\Gamma_1 \ni \sigma, \Gamma_1 \ni \sigma' \\ \Gamma_2 = \Gamma_1 \cup \sigma'}} \frac{\sqrt{m_{\Gamma_1} m_{\Gamma_2}}}{(1 - n_{f\sigma}^0) \sqrt{n_{f\sigma'}^0 (1 - n_{f\sigma'}^0)}}
\end{aligned}$$

and

$$\begin{aligned}
B_{\sigma\sigma'}^{++} &= \sum_{\Gamma \ni \sigma, \Gamma \ni \sigma'} \frac{m_{\Gamma}}{n_{f\sigma}^0 n_{f\sigma'}^0} \\
B_{\sigma\sigma'}^{+-} &= \sum_{\Gamma \ni \sigma, \Gamma \ni \sigma'} \frac{m_{\Gamma}}{n_{f\sigma}^0 (1 - n_{f\sigma'}^0)} \\
B_{\sigma\sigma'}^{--} &= \sum_{\Gamma \ni \sigma, \Gamma \ni \sigma'} \frac{m_{\Gamma}}{(1 - n_{f\sigma}^0) (1 - n_{f\sigma'}^0)}
\end{aligned}$$

we will have

$$\begin{aligned}
\langle +k_1\sigma \mid \hat{H}_{band} \mid +k_2\sigma \rangle &= \sum_{k'\sigma'} \epsilon_{k'\sigma'} [\delta_{\sigma\sigma'} \langle 0 \mid \hat{c}_{k_1\sigma} \hat{c}_{k'\sigma}^+ \hat{c}_{k'\sigma} \hat{c}_{k_2\sigma}^+ \mid 0 \rangle \\
&\quad + (1 - \delta_{\sigma\sigma'}) \\
&\quad \times (B_{\sigma\sigma'}^{++} \langle 0 \mid \hat{c}_{k_1\sigma} \hat{c}_{k_2\sigma}^+ \hat{f}_{\sigma}^{\dagger} \hat{f}_{\sigma} \mid 0 \rangle \langle 0 \mid \hat{c}_{k'\sigma'}^+ \hat{c}_{k'\sigma'} \hat{f}_{\sigma'}^{\dagger} \hat{f}_{\sigma'} \mid 0 \rangle \\
&\quad + B_{\sigma\sigma'}^{+-} \langle 0 \mid \hat{c}_{k_1\sigma} \hat{c}_{k_2\sigma}^+ \hat{f}_{\sigma}^{\dagger} \hat{f}_{\sigma} \mid 0 \rangle \langle 0 \mid \hat{c}_{k'\sigma'}^+ \hat{c}_{k'\sigma'} \hat{f}_{\sigma'}^{\dagger} \hat{f}_{\sigma'} \mid 0 \rangle \\
&\quad + B_{\sigma'\sigma}^{+-} \langle 0 \mid \hat{c}_{k_1\sigma} \hat{c}_{k_2\sigma}^+ \hat{f}_{\sigma} \hat{f}_{\sigma}^{\dagger} \mid 0 \rangle \langle 0 \mid \hat{c}_{k'\sigma'}^+ \hat{c}_{k'\sigma'} \hat{f}_{\sigma'}^{\dagger} \hat{f}_{\sigma'} \mid 0 \rangle \\
&\quad + B_{\sigma\sigma'}^{--} \langle 0 \mid \hat{c}_{k_1\sigma} \hat{c}_{k_2\sigma}^+ \hat{f}_{\sigma} \hat{f}_{\sigma}^{\dagger} \mid 0 \rangle \langle 0 \mid \hat{c}_{k'\sigma'}^+ \hat{c}_{k'\sigma'} \hat{f}_{\sigma'}^{\dagger} \hat{f}_{\sigma'} \mid 0 \rangle)
\end{aligned}$$

$$\begin{aligned} \langle +k\sigma | \hat{H}_{band} | UHB \rangle &= \sum_{k'\sigma'} \epsilon_{k'\sigma'} [\delta_{\sigma\sigma'} z_\sigma \langle 0 | \hat{c}_{k\sigma} \hat{c}_{k'\sigma}^+ \hat{c}_{k'\sigma} \hat{f}_\sigma^\dagger | 0 \rangle \\ &\quad + (1 - \delta_{\sigma\sigma'}) \langle 0 | \hat{c}_{k\sigma} \hat{f}_\sigma^\dagger | 0 \rangle (x_{\sigma'\sigma} \langle 0 | \hat{c}_{k'\sigma}^+ \hat{c}_{k'\sigma'} \hat{f}_{\sigma'}^\dagger \hat{f}_{\sigma'} | 0 \rangle + v_{\sigma'\sigma} \langle 0 | \hat{c}_{k'\sigma}^+ \hat{c}_{k'\sigma'} \hat{f}_{\sigma'} \hat{f}_{\sigma'}^\dagger | 0 \rangle)] \end{aligned}$$

$$\begin{aligned} \langle +k\sigma | \hat{H}_{band} | QE \rangle &= \sum_{k'\sigma'} \epsilon_{k'\sigma'} [\delta_{\sigma\sigma'} \langle 0 | \hat{c}_{k\sigma} \hat{c}_{k'\sigma}^+ \hat{c}_{k'\sigma} \hat{f}_\sigma^\dagger | 0 \rangle \\ &\quad + (1 - \delta_{\sigma\sigma'}) \langle 0 | \hat{c}_{k\sigma} \hat{f}_\sigma^\dagger | 0 \rangle (B_{\sigma\sigma'}^{++} \langle 0 | \hat{c}_{k'\sigma}^+ \hat{c}_{k'\sigma'} \hat{f}_{\sigma'}^\dagger \hat{f}_{\sigma'} | 0 \rangle + B_{\sigma\sigma'}^{+-} \langle 0 | \hat{c}_{k'\sigma}^+ \hat{c}_{k'\sigma'} \hat{f}_{\sigma'} \hat{f}_{\sigma'}^\dagger | 0 \rangle)] \end{aligned}$$

$$\begin{aligned} \langle UHB | \hat{H}_{band} | UHB \rangle &= \sum_{k'\sigma'} \epsilon_{k'\sigma'} [\delta_{\sigma\sigma'} \langle 0 | \hat{f}_\sigma \hat{c}_{k'\sigma}^+ \hat{c}_{k'\sigma} \hat{f}_\sigma^\dagger | 0 \rangle \\ &\quad + (1 - \delta_{\sigma\sigma'}) (1 - n_{f\sigma}^0) \\ &\quad \times (B_{\sigma\sigma'}^{+-} \langle 0 | \hat{c}_{k'\sigma}^+ \hat{c}_{k'\sigma'} \hat{f}_{\sigma'}^\dagger \hat{f}_{\sigma'} | 0 \rangle + B_{\sigma\sigma'}^{--} \langle 0 | \hat{c}_{k'\sigma}^+ \hat{c}_{k'\sigma'} \hat{f}_{\sigma'} \hat{f}_{\sigma'}^\dagger | 0 \rangle)] \end{aligned}$$

$$\begin{aligned} \langle UHB | \hat{H}_{band} | QE \rangle &= \sum_{k'\sigma'} \epsilon_{k'\sigma'} [\delta_{\sigma\sigma'} z_\sigma \langle 0 | \hat{f}_\sigma \hat{c}_{k'\sigma}^+ \hat{c}_{k'\sigma} \hat{f}_\sigma^\dagger | 0 \rangle \\ &\quad + (1 - \delta_{\sigma\sigma'}) (1 - n_{f\sigma}^0) \\ &\quad \times (x_{\sigma'\sigma} \langle 0 | \hat{c}_{k'\sigma}^+ \hat{c}_{k'\sigma'} \hat{f}_{\sigma'}^\dagger \hat{f}_{\sigma'} | 0 \rangle + v_{\sigma'\sigma} \langle 0 | \hat{c}_{k'\sigma}^+ \hat{c}_{k'\sigma'} \hat{f}_{\sigma'} \hat{f}_{\sigma'}^\dagger | 0 \rangle)] \end{aligned}$$

$$\begin{aligned} \langle QE | \hat{H}_{band} | QE \rangle &= \sum_{k'\sigma'} \epsilon_{k'\sigma'} [\delta_{\sigma\sigma'} \langle 0 | \hat{f}_\sigma \hat{c}_{k'\sigma}^+ \hat{c}_{k'\sigma} \hat{f}_\sigma^\dagger | 0 \rangle \\ &\quad + (1 - \delta_{\sigma\sigma'}) (1 - n_{f\sigma}^0) \\ &\quad \times (B_{\sigma\sigma'}^{++} \langle 0 | \hat{c}_{k'\sigma}^+ \hat{c}_{k'\sigma'} \hat{f}_{\sigma'}^\dagger \hat{f}_{\sigma'} | 0 \rangle + B_{\sigma\sigma'}^{+-} \langle 0 | \hat{c}_{k'\sigma}^+ \hat{c}_{k'\sigma'} \hat{f}_{\sigma'} \hat{f}_{\sigma'}^\dagger | 0 \rangle)] \end{aligned}$$

$$\begin{aligned} \langle -k_1\sigma | \hat{H}_{band} | -k_2\sigma \rangle &= \sum_{k'\sigma'} \epsilon_{k'\sigma'} [\delta_{\sigma\sigma'} \langle 0 | \hat{c}_{k_1\sigma}^+ \hat{c}_{k'\sigma}^+ \hat{c}_{k'\sigma} \hat{c}_{k_2\sigma} | 0 \rangle \\ &\quad + (1 - \delta_{\sigma\sigma'}) \\ &\quad \times (B_{\sigma\sigma'}^{++} \langle 0 | \hat{c}_{k_1\sigma}^+ \hat{c}_{k_2\sigma} \hat{f}_\sigma^\dagger \hat{f}_\sigma | 0 \rangle \langle 0 | \hat{c}_{k'\sigma}^+ \hat{c}_{k'\sigma'} \hat{f}_{\sigma'}^\dagger \hat{f}_{\sigma'} | 0 \rangle \\ &\quad + B_{\sigma\sigma'}^{+-} \langle 0 | \hat{c}_{k_1\sigma}^+ \hat{c}_{k_2\sigma} \hat{f}_\sigma^\dagger \hat{f}_\sigma | 0 \rangle \langle 0 | \hat{c}_{k'\sigma}^+ \hat{c}_{k'\sigma'} \hat{f}_{\sigma'} \hat{f}_{\sigma'}^\dagger | 0 \rangle \\ &\quad + B_{\sigma\sigma'}^{-+} \langle 0 | \hat{c}_{k_1\sigma}^+ \hat{c}_{k_2\sigma} \hat{f}_\sigma \hat{f}_\sigma^\dagger | 0 \rangle \langle 0 | \hat{c}_{k'\sigma}^+ \hat{c}_{k'\sigma'} \hat{f}_{\sigma'}^\dagger \hat{f}_{\sigma'} | 0 \rangle \\ &\quad + B_{\sigma\sigma'}^{--} \langle 0 | \hat{c}_{k_1\sigma}^+ \hat{c}_{k_2\sigma} \hat{f}_\sigma \hat{f}_\sigma^\dagger | 0 \rangle \langle 0 | \hat{c}_{k'\sigma}^+ \hat{c}_{k'\sigma'} \hat{f}_{\sigma'} \hat{f}_{\sigma'}^\dagger | 0 \rangle)] \end{aligned}$$

$$\begin{aligned} \langle -k\sigma | \hat{H}_{band} | LHB \rangle &= \sum_{k'\sigma'} \epsilon_{k'\sigma'} (\delta_{\sigma\sigma'} z_\sigma \langle 0 | \hat{c}_{k\sigma}^+ \hat{c}_{k'\sigma}^+ \hat{c}_{k'\sigma} \hat{f}_\sigma | 0 \rangle \\ &\quad + (1 - \delta_{\sigma\sigma'}) \langle 0 | \hat{c}_{k\sigma}^+ \hat{f}_\sigma | 0 \rangle (x_{\sigma'\sigma} \langle 0 | \hat{c}_{k'\sigma'}^+ \hat{c}_{k'\sigma'} \hat{f}_{\sigma'}^\dagger \hat{f}_{\sigma'} | 0 \rangle + v_{\sigma'\sigma} \langle 0 | \hat{c}_{k'\sigma'}^+ \hat{c}_{k'\sigma'} \hat{f}_{\sigma'} \hat{f}_{\sigma'}^\dagger | 0 \rangle)) \end{aligned}$$

$$\begin{aligned} \langle -k\sigma | \hat{H}_{band} | QH \rangle &= \sum_{k'\sigma'} \epsilon_{k'\sigma'} (\delta_{\sigma\sigma'} \langle 0 | \hat{c}_{k\sigma}^+ \hat{c}_{k'\sigma}^+ \hat{c}_{k'\sigma} \hat{f}_\sigma | 0 \rangle \\ &\quad + (1 - \delta_{\sigma\sigma'}) \langle 0 | \hat{c}_{k\sigma}^+ \hat{f}_\sigma | 0 \rangle (B_{\sigma\sigma'}^{-+} \langle 0 | \hat{c}_{k'\sigma'}^+ \hat{c}_{k'\sigma'} \hat{f}_{\sigma'}^\dagger \hat{f}_{\sigma'} | 0 \rangle + B_{\sigma\sigma'}^{--} \langle 0 | \hat{c}_{k'\sigma'}^+ \hat{c}_{k'\sigma'} \hat{f}_{\sigma'} \hat{f}_{\sigma'}^\dagger | 0 \rangle)) \end{aligned}$$

$$\begin{aligned} \langle LHB | \hat{H}_{band} | LHB \rangle &= \sum_{k'\sigma'} \epsilon_{k'\sigma'} [\delta_{\sigma\sigma'} \langle 0 | \hat{f}_\sigma^\dagger \hat{c}_{k'\sigma}^+ \hat{c}_{k'\sigma} \hat{f}_\sigma | 0 \rangle \\ &\quad + (1 - \delta_{\sigma\sigma'}) n_{f_\sigma}^0 \\ &\quad \times (B_{\sigma\sigma'}^{++} \langle 0 | \hat{c}_{k'\sigma'}^+ \hat{c}_{k'\sigma'} \hat{f}_{\sigma'}^\dagger \hat{f}_{\sigma'} | 0 \rangle + B_{\sigma\sigma'}^{+-} \langle 0 | \hat{c}_{k'\sigma'}^+ \hat{c}_{k'\sigma'} \hat{f}_{\sigma'} \hat{f}_{\sigma'}^\dagger | 0 \rangle)] \end{aligned}$$

$$\begin{aligned} \langle LHB | \hat{H}_{band} | QH \rangle &= \sum_{k'\sigma'} \epsilon_{k'\sigma'} [\delta_{\sigma\sigma'} z_\sigma \langle 0 | \hat{f}_\sigma^\dagger \hat{c}_{k'\sigma}^+ \hat{c}_{k'\sigma} \hat{f}_\sigma | 0 \rangle \\ &\quad + (1 - \delta_{\sigma\sigma'}) n_{f_\sigma}^0 \\ &\quad \times (x_{\sigma'\sigma} \langle 0 | \hat{c}_{k'\sigma'}^+ \hat{c}_{k'\sigma'} \hat{f}_{\sigma'}^\dagger \hat{f}_{\sigma'} | 0 \rangle + v_{\sigma'\sigma} \langle 0 | \hat{c}_{k'\sigma'}^+ \hat{c}_{k'\sigma'} \hat{f}_{\sigma'} \hat{f}_{\sigma'}^\dagger | 0 \rangle)] \end{aligned}$$

$$\begin{aligned} \langle QH | \hat{H}_{band} | QH \rangle &= \sum_{k'\sigma'} \epsilon_{k'\sigma'} [\delta_{\sigma\sigma'} \langle 0 | \hat{f}_\sigma^\dagger \hat{c}_{k'\sigma}^+ \hat{c}_{k'\sigma} \hat{f}_\sigma | 0 \rangle \\ &\quad + (1 - \delta_{\sigma\sigma'}) n_{f_\sigma}^0 \\ &\quad \times (B_{\sigma\sigma'}^{-+} \langle 0 | \hat{c}_{k'\sigma'}^+ \hat{c}_{k'\sigma'} \hat{f}_{\sigma'}^\dagger \hat{f}_{\sigma'} | 0 \rangle + B_{\sigma\sigma'}^{--} \langle 0 | \hat{c}_{k'\sigma'}^+ \hat{c}_{k'\sigma'} \hat{f}_{\sigma'} \hat{f}_{\sigma'}^\dagger | 0 \rangle)] \end{aligned}$$

## 2. $H_{local}$

Here we define a function for set:

$$A_{\sigma,\Gamma} = \begin{cases} 1, & \text{if } \sigma \in \Gamma \\ 0, & \text{if } \sigma \notin \Gamma \end{cases}$$



then define

$$S_\Gamma = E_\Gamma + \sum_{\sigma'} \varepsilon_{\sigma'} A_{\sigma', \Gamma}$$

and

$$\begin{aligned} S_1 &= \sum_{\Gamma} E_\Gamma m_\Gamma + \sum_{\sigma'} \varepsilon_{\sigma'} \sum_{\Gamma \ni \sigma'} m_\Gamma \\ &= \sum_{\Gamma} m_\Gamma S_\Gamma \end{aligned}$$

$$\begin{aligned} S_2(\sigma) &= \sum_{\Gamma} E_\Gamma A_{\sigma, \Gamma} \sqrt{m_\Gamma m_{\Gamma \setminus \sigma}} + \sum_{\sigma'} \varepsilon_{\sigma'} \sum_{\Gamma \ni \sigma'} A_{\sigma, \Gamma} \sqrt{m_\Gamma m_{\Gamma \setminus \sigma}} \\ &= \sum_{\Gamma} A_{\sigma, \Gamma} \sqrt{m_\Gamma m_{\Gamma \setminus \sigma}} S_\Gamma \end{aligned}$$

$$\begin{aligned} S_3(\sigma) &= \sum_{\Gamma} E_\Gamma A_{\sigma, \Gamma} m_\Gamma + \sum_{\sigma'} \varepsilon_{\sigma'} \sum_{\Gamma \ni \sigma'} A_{\sigma, \Gamma} m_\Gamma \\ &= \sum_{\Gamma} A_{\sigma, \Gamma} m_\Gamma S_\Gamma \end{aligned}$$

$$\begin{aligned} S_4(\sigma) &= \sum_{\Gamma} E_\Gamma A_{\sigma, \Gamma} m_{\Gamma \setminus \sigma} + \sum_{\sigma'} \varepsilon_{\sigma'} \sum_{\Gamma \ni \sigma'} A_{\sigma, \Gamma} m_{\Gamma \setminus \sigma} \\ &= \sum_{\Gamma} A_{\sigma, \Gamma} m_{\Gamma \setminus \sigma} S_\Gamma \end{aligned}$$

$$\begin{aligned} S_5(\sigma) &= \sum_{\Gamma} E_\Gamma (1 - A_{\sigma, \Gamma}) \sqrt{m_\Gamma m_{\Gamma \cup \sigma}} + \sum_{\sigma'} \varepsilon_{\sigma'} \sum_{\Gamma \ni \sigma'} (1 - A_{\sigma, \Gamma}) \sqrt{m_\Gamma m_{\Gamma \cup \sigma}} \\ &= \sum_{\Gamma} (1 - A_{\sigma, \Gamma}) \sqrt{m_\Gamma m_{\Gamma \cup \sigma}} S_\Gamma \end{aligned}$$

$$\begin{aligned} S_6(\sigma) &= \sum_{\Gamma} E_\Gamma (1 - A_{\sigma, \Gamma}) m_\Gamma + \sum_{\sigma'} \varepsilon_{\sigma'} \sum_{\Gamma \ni \sigma'} (1 - A_{\sigma, \Gamma}) m_\Gamma \\ &= \sum_{\Gamma} (1 - A_{\sigma, \Gamma}) m_\Gamma S_\Gamma \end{aligned}$$

$$\begin{aligned} S_7(\sigma) &= \sum_{\Gamma} E_\Gamma (1 - A_{\sigma, \Gamma}) m_{\Gamma \cup \sigma} + \sum_{\sigma'} \varepsilon_{\sigma'} \sum_{\Gamma \ni \sigma'} (1 - A_{\sigma, \Gamma}) m_{\Gamma \cup \sigma} \\ &= \sum_{\Gamma} (1 - A_{\sigma, \Gamma}) m_{\Gamma \cup \sigma} S_\Gamma \end{aligned}$$

$$\begin{aligned}
S_{25}(\sigma) &= \sum_{\Gamma} E_{\Gamma} \left[ A_{\sigma, \Gamma} \frac{m_{\Gamma}}{n_{f\sigma}^0} - (1 - A_{\sigma, \Gamma}) \frac{m_{\Gamma}}{1 - n_{f\sigma}^0} \right] \\
&\quad + \sum_{\sigma'} \varepsilon_{\sigma'} \sum_{\Gamma \ni \sigma'} A_{\sigma', \Gamma} \left[ A_{\sigma, \Gamma} \frac{m_{\Gamma}}{n_{f\sigma}^0} - (1 - A_{\sigma, \Gamma}) \frac{m_{\Gamma}}{1 - n_{f\sigma}^0} \right] \\
&= \left[ A_{\sigma, \Gamma} \frac{m_{\Gamma}}{n_{f\sigma}^0} - (1 - A_{\sigma, \Gamma}) \frac{m_{\Gamma}}{1 - n_{f\sigma}^0} \right] S_{\Gamma}
\end{aligned}$$

thus

$$\langle +k_1\sigma \mid \hat{H}_{local} \mid +k_2\sigma \rangle = \langle 0 \mid \hat{c}_{k_1\sigma} \hat{c}_{k_2\sigma}^+ \mid 0 \rangle S_1 + \langle 0 \mid \hat{c}_{k_1\sigma} \hat{f}_{\sigma}^{\dagger} \mid 0 \rangle \langle 0 \mid \hat{f}_{\sigma} \hat{c}_{k_2\sigma}^+ \mid 0 \rangle S_{25}(\sigma)$$

$$\langle +k\sigma \mid \hat{H}_{local} \mid UHB \rangle = \frac{1}{\sqrt{n_{f\sigma}^0(1 - n_{f\sigma}^0)}} \langle 0 \mid \hat{c}_{k\sigma} \hat{f}_{\sigma}^{\dagger} \mid 0 \rangle S_2(\sigma)$$

$$\langle +k\sigma \mid \hat{H}_{local} \mid QE \rangle = \frac{1}{n_{f\sigma}^0} \langle 0 \mid \hat{c}_{k\sigma} \hat{f}_{\sigma}^{\dagger} \mid 0 \rangle S_3(\sigma)$$

$$\langle UHB \mid \hat{H}_{local} \mid UHB \rangle = S_4(\sigma)$$

$$\langle UHB \mid \hat{H}_{local} \mid QE \rangle = \frac{\sqrt{1 - n_{f\sigma}^0}}{\sqrt{n_{f\sigma}^0}} S_2(\sigma)$$

$$\langle QE \mid \hat{H}_{local} \mid QE \rangle = \frac{1 - n_{f\sigma}^0}{n_{f\sigma}^0} S_3(\sigma)$$

$$\langle -k_1\sigma \mid \hat{H}_{local} \mid -k_2\sigma \rangle = \langle 0 \mid \hat{c}_{k_1\sigma}^+ \hat{c}_{k_2\sigma} \mid 0 \rangle S_1 - \langle 0 \mid \hat{c}_{k_1\sigma}^+ \hat{f}_{\sigma} \mid 0 \rangle \langle 0 \mid \hat{f}_{\sigma} \hat{c}_{k_2\sigma} \mid 0 \rangle S_{25}(\sigma)$$

$$\langle -k\sigma \mid \hat{H}_{local} \mid LHB \rangle = \frac{1}{\sqrt{n_{f\sigma}^0(1 - n_{f\sigma}^0)}} \langle 0 \mid \hat{c}_{k\sigma}^+ \hat{f}_{\sigma} \mid 0 \rangle S_5(\sigma)$$

$$\langle -k\sigma \mid \hat{H}_{local} \mid QH \rangle = \frac{1}{1 - n_{f\sigma}^0} \langle 0 \mid \hat{c}_{k\sigma}^+ \hat{f}_{\sigma} \mid 0 \rangle S_6(\sigma)$$

$$\langle LHB \mid \hat{H}_{local} \mid LHB \rangle = S_7(\sigma)$$

$$\langle LHB \mid \hat{H}_{local} \mid QH \rangle = \frac{\sqrt{n_{f\sigma}^0}}{\sqrt{1 - n_{f\sigma}^0}} S_5(\sigma)$$

$$\langle QH|\hat{H}_{local}|QH\rangle = \frac{n_{f\sigma}^0}{1-n_{f\sigma}^0}S_6(\sigma)$$

### 3. $H_V$

$$\begin{aligned} \langle +k_1\sigma|\hat{H}_V|+k_2\sigma\rangle &= \sum_{k'\sigma'} V_{k'\sigma'}[\delta_{\sigma\sigma'}z_\sigma(\langle 0|\hat{c}_{k_1\sigma}\hat{c}_{k'\sigma}^+\hat{f}_\sigma\hat{c}_{k_2\sigma}^+|0\rangle + \langle 0|\hat{c}_{k_1\sigma}\hat{f}_\sigma^\dagger\hat{c}_{k'\sigma}\hat{c}_{k_2\sigma}^+|0\rangle) \\ &\quad + (1-\delta_{\sigma\sigma'}) (\langle 0|\hat{c}_{k'\sigma}^+\hat{f}_{\sigma'}|0\rangle + \langle 0|\hat{f}_{\sigma'}^\dagger\hat{c}_{k'\sigma}|0\rangle) \\ &\quad \times (x_{\sigma\sigma'}\langle 0|\hat{c}_{k_1\sigma}\hat{c}_{k_2\sigma}^+\hat{f}_\sigma^\dagger\hat{f}_\sigma|0\rangle + v_{\sigma\sigma'}\langle 0|\hat{c}_{k_1\sigma}\hat{c}_{k_2\sigma}^+\hat{f}_\sigma\hat{f}_\sigma^\dagger|0\rangle)] \end{aligned}$$

$$\begin{aligned} \langle +k\sigma|\hat{H}_V|UHB\rangle &= \sum_{k'\sigma'} V_{k'\sigma'}[\delta_{\sigma\sigma'}\langle 0|\hat{c}_{k\sigma}\hat{c}_{k'\sigma}^+\hat{f}_\sigma\hat{f}_\sigma^\dagger|0\rangle \\ &\quad + (1-\delta_{\sigma\sigma'})\langle 0|\hat{c}_{k\sigma}\hat{f}_\sigma^\dagger|0\rangle (y_{\sigma\sigma'}\langle 0|\hat{c}_{k'\sigma}^+\hat{f}_{\sigma'}|0\rangle + w_{\sigma\sigma'}\langle 0|\hat{f}_{\sigma'}^\dagger\hat{c}_{k'\sigma}|0\rangle)] \end{aligned}$$

$$\begin{aligned} \langle +k\sigma|\hat{H}_V|QE\rangle &= \sum_{k'\sigma'} V_{k'\sigma'}[\delta_{\sigma\sigma'}z_\sigma\langle 0|\hat{c}_{k\sigma}\hat{c}_{k'\sigma}^+\hat{f}_\sigma\hat{f}_\sigma^\dagger|0\rangle \\ &\quad + (1-\delta_{\sigma\sigma'})x_{\sigma\sigma'}\langle 0|\hat{c}_{k\sigma}\hat{f}_\sigma^\dagger|0\rangle (\langle 0|\hat{c}_{k'\sigma}^+\hat{f}_{\sigma'}|0\rangle + \langle 0|\hat{f}_{\sigma'}^\dagger\hat{c}_{k'\sigma}|0\rangle)] \end{aligned}$$

$$\langle UHB|\hat{H}_V|UHB\rangle = \sum_{k'\sigma'} V_{k'\sigma'}(1-\delta_{\sigma\sigma'})v_{\sigma\sigma'}(1-n_{f\sigma}^0)(\langle 0|\hat{c}_{k'\sigma}^+\hat{f}_{\sigma'}|0\rangle + \langle 0|\hat{f}_{\sigma'}^\dagger\hat{c}_{k'\sigma}|0\rangle)$$

$$\langle UHB|\hat{H}_V|QE\rangle = \sum_{k'\sigma'} V_{k'\sigma'}(1-\delta_{\sigma\sigma'})(1-n_{f\sigma}^0)(w_{\sigma\sigma'}\langle 0|\hat{c}_{k'\sigma}^+\hat{f}_{\sigma'}|0\rangle + y_{\sigma\sigma'}\langle 0|\hat{f}_{\sigma'}^\dagger\hat{c}_{k'\sigma}|0\rangle)$$

$$\langle QE|\hat{H}_V|QE\rangle = \sum_{k'\sigma'} V_{k'\sigma'}(1-\delta_{\sigma\sigma'})x_{\sigma\sigma'}(1-n_{f\sigma}^0)(\langle 0|\hat{c}_{k'\sigma}^+\hat{f}_{\sigma'}|0\rangle + \langle 0|\hat{f}_{\sigma'}^\dagger\hat{c}_{k'\sigma}|0\rangle)$$

$$\begin{aligned}
\langle -k_1\sigma | \hat{H}_V | -k_2\sigma \rangle &= \sum_{k'\sigma'} V_{k'\sigma'} [\delta_{\sigma\sigma'} z_\sigma (\langle 0 | \hat{c}_{k_1\sigma}^+ \hat{c}_{k'\sigma}^+ \hat{f}_\sigma \hat{c}_{k_2\sigma} | 0 \rangle + \langle 0 | \hat{c}_{k_1\sigma}^+ \hat{f}_\sigma^\dagger \hat{c}_{k'\sigma} \hat{c}_{k_2\sigma} | 0 \rangle) \\
&\quad + (1 - \delta_{\sigma\sigma'}) (\langle 0 | \hat{c}_{k'\sigma'}^+ \hat{f}_{\sigma'} | 0 \rangle + \langle 0 | \hat{f}_{\sigma'}^\dagger \hat{c}_{k'\sigma'} | 0 \rangle) \\
&\quad (x_{\sigma\sigma'} \langle 0 | \hat{c}_{k_1\sigma}^+ \hat{c}_{k_2\sigma} \hat{f}_\sigma^\dagger \hat{f}_\sigma | 0 \rangle + v_{\sigma\sigma'} \langle 0 | \hat{c}_{k_1\sigma}^+ \hat{c}_{k_2\sigma} \hat{f}_\sigma \hat{f}_\sigma^\dagger | 0 \rangle)]
\end{aligned}$$

$$\begin{aligned}
\langle -k\sigma | \hat{H}_V | LHB \rangle &= \sum_{k'\sigma'} V_{k'\sigma'} [\delta_{\sigma\sigma'} \langle 0 | \hat{c}_{k\sigma}^+ \hat{f}_\sigma^\dagger \hat{c}_{k'\sigma} \hat{f}_\sigma | 0 \rangle \\
&\quad + (1 - \delta_{\sigma\sigma'}) \langle 0 | \hat{c}_{k\sigma}^+ \hat{f}_\sigma | 0 \rangle (w_{\sigma\sigma'} \langle 0 | \hat{c}_{k'\sigma'}^+ \hat{f}_{\sigma'} | 0 \rangle + y_{\sigma\sigma'} \langle 0 | \hat{f}_{\sigma'}^\dagger \hat{c}_{k'\sigma'} | 0 \rangle)]
\end{aligned}$$

$$\begin{aligned}
\langle -k\sigma | H_V | QH \rangle &= \sum_{k'\sigma'} V_{k'\sigma'} [\delta_{\sigma\sigma'} z_\sigma \langle 0 | c_{k\sigma}^+ f_\sigma^\dagger c_{k'\sigma} f_\sigma | 0 \rangle \\
&\quad + (1 - \delta_{\sigma\sigma'}) v_{\sigma\sigma'} \langle 0 | c_{k\sigma}^+ f_\sigma | 0 \rangle (\langle 0 | c_{k'\sigma'}^+ f_{\sigma'} | 0 \rangle + \langle 0 | f_{\sigma'}^\dagger c_{k'\sigma'} | 0 \rangle)]
\end{aligned}$$

$$\langle LHB | \hat{H}_V | LHB \rangle = \sum_{k'\sigma'} V_{k'\sigma'} (1 - \delta_{\sigma\sigma'}) x_{\sigma\sigma'} n_{f\sigma}^0 (\langle 0 | \hat{c}_{k'\sigma'}^+ \hat{f}_{\sigma'} | 0 \rangle + \langle 0 | \hat{f}_{\sigma'}^\dagger \hat{c}_{k'\sigma'} | 0 \rangle)$$

$$\langle LHB | H_V | QH \rangle = \sum_{k'\sigma'} V_{k'\sigma'} (1 - \delta_{\sigma\sigma'}) n_{f\sigma}^0 (y_{\sigma\sigma'} \langle 0 | c_{k'\sigma'}^+ f_{\sigma'} | 0 \rangle + w_{\sigma\sigma'} \langle 0 | f_{\sigma'}^\dagger c_{k'\sigma'} | 0 \rangle)$$

$$\langle QH | H_V | QH \rangle = \sum_{k'\sigma'} V_{k'\sigma'} (1 - \delta_{\sigma\sigma'}) v_{\sigma\sigma'} n_{f\sigma}^0 (\langle 0 | c_{k'\sigma'}^+ f_{\sigma'} | 0 \rangle + \langle 0 | f_{\sigma'}^\dagger c_{k'\sigma'} | 0 \rangle)$$

---

[1] Hohenberg P and Kohn W 1964 *Phys. Rev.* **136** B864.

Kohn W and Sham L J 1965 *Phys. Rev.* **140** A1133.

[2] Anisimov V I, Zaanen J and Andersen O K 1991 *Phys. Rev. B* **44** 943.

[3] Anisimov V I, Aryasetiawan F and Lichtensten A I 1997 *J.Phys.: Condens. Matter* **9** 767.

[4] Mott, N. F., 1949, *Proc. Phys. Soc. A* **62**, 416.

[5] Mott, N. F., 1956, *Can. J. Phys.* **34**, 1356.

- [6] Mott, N. F., 1961, *Philos. Mag.* **6**, 287.
- [7] Gutzwiller, M. C., 1965, *Phys. Rev.* **137**, A1726.
- [8] Dieter Vollhardt, *Rev. Mod. Phys.* Vol. 56, No. 1, January 1984.
- [9] J. Bünemann, W. Weber and F. Gebhard, *Physical Review B*, **57**, 12 (1998).
- [10] Xiaoyu Deng, Xi Dai and Zhong Fang, *EPL*, **83** (2008) 37008.
- [11] Xiaoyu Deng et al, unpublished.
- [12] Georges A, Kotliar G, Krauth W and Rozenberg M J, 1996 *Rev. Mod. Phys.* **68** 13.
- [13] Mott, N. F., 1990, *Metal Insulator Transitions* (Taylor and Francis, London.)
- [14] Tsuda, N., K. Nasu, A. Yanase, and K. Siratori, 1991, *Electronic Conduction in Oxides*, Springer Series in Solid State Sciences Vol. 94 (Springer-Verlag, Berlin).
- [15] M. Jarrell, Th. Maier, M. H. Hettler and A. N. Tahvildarzadeh, *Phys. Rev. Lett.* **98**, 016402 (2007).
- [16] Qimiao Si, Silvio Rabello, Kevin Ingersent and J. Llewellyn Smith, *Nature* **413**, 804 - 808 (25 Oct 2001).
- [17] Philipp Gegenwart, Qimiao Si and Frank Steglich, arXiv:0712.2045v2.
- [18] V I Anisimov, A I Poteryaev, M A Korotin, A O Anokhin and G Kotliar 1997 *J.Phys.: Condens. Matter* **9** 7359.
- [19] Dai. X, S. Y. Savrasov, G. Kotliar, A. Migliori, H. Ledbetter, and E. Abrahams, 2003, *Science* **300**, 953.
- [20] J. H. Shim, K. Haule, G. Kotliar, 1 November 2007/ Page 3/10.1126/science.1149064.
- [21] G. Kotliar, S. Y. Savrasov, K. Haule, V. S. Oudovenko, O. Parcollet and C. A. Marianetti, *Rev. Mod. Phys.* **78** 865 (2006).
- [22] K. Held, eprint: cond-mat/0511293 unpublished.
- [23] H. O. Jeschke and G. Kotliar *Phys. Rev. B* **71**, 085103(2005).
- [24] S. Y. Savrasov, V. Oudovenko, K. Haule, D. Villani, G. Kotliar, arXiv:cond-mat/0410410v1.
- [25] M.J. Han, X. Wan, S.Y. Savrasov, arXiv:0806.0408v1.
- [26] M. J. Rozenberg, G. Kotliar, and X. Y. Zhang, *Phys. Rev. B* **49**, 10181(1994).
- [27] S. Y. Savrasov, V. Oudovenko, K. Haule, D. Villani, and G. Kotliar *Phys. Rev. B* **71**, 115117(2005).
- [28] M. Jarrell, and Th. Pruschke, *Phys. Rev. B* **49**, 1458 (1994); K. Haule, V. Oudovenko, S. Y. Savrasov, and G. Kotliar, *Phys. Rev. Lett.* **94**, 036401 (2005).

- [29] L. Chioncel, L. Vitos, I. A. Abrikosov, J. Kollr, M. I. Katsnelson, and A. I. Lichtenstein, Phys. Rev. B **67**, 235106(2003); V. Drchal, V. Janiš, J. Kudrnovsk, V. S. Oudovenko, X. Dai, K. Haule, and G. Kotliar, J. Phys.: Cond. Matt. **17**, 61 (2005).
- [30] Michel Caffarel and Werner Krauth, Physical Review Letters **72**, 10.
- [31] L. Laloux, A. Georges, and W. Krauth, Phys. Rev. B **50**, 3092(1994).
- [32] Hirsch, J. E., and R. M. Fye, 1986, Phys. Rev. Lett. **56**, 2521.
- [33] R. Bulla, A. C. Hewson and Th. Pruschke, J. Phys.: Condens. Matter **10** (1998) 8365-8380.
- [34] P. Werner, A. Comanac, L. de' Medici, M. Troyer, and A. J. Millis, Physical Review Letter **97**, 076405 (2006).
- [35] A. N. Rubtsov, V. V. Savkin, and A. I. Lichtenstein<sup>3</sup>, PRB, **72** 035122(2005).
- [36] X. Dai, S. Y. Savrasov, G. Kotliar, A. Migliori, H. Ledbetter, and E. Abrahams, Science 9 May 2003 **300**: 953-955.
- [37] K. Haule, J. H. Shim and G. Kotliar, Phys. Rev. Lett. **100**, 226402 (2008).
- [38] T. M. Rice & K. Ueda, Phys. Rev. B **34**, 9 (1986).
- [39] Shiba, H. & Fazekas, P. (1990). *Prog. Theor. Phys. Suppl.* **101**, 403.
- [40] Fei Tan, Qiang-Hua Wang, Phys. Rev. Lett. **100**, 117004 (2008).
- [41] X. Dai , G. Kotliar and Z. Fang eprint : cond-mat/0611075.
- [42] A. L. Fetter and J. D. Walecka, *Quantum Theory of Many-Particle Systems* (McGraw-Hill, New York, 1971).
- [43] O. Gunnarsson and K. Schönhammer, Phys. Rev. B **28**, 8 (1983).
- [44] A. C. Hewson, *The Kondo Problem to Heavy Fermions*, Cambridge university press
- [45] S. Sugano, Y. Tanabe, and H. Kamimura, *Multiplets of Transition-Metal Ions in Crystals*, Pure and Applied Physics Vol.33 (Academic New York, 1970).
- [46] Kensuke Inaba and Akihisa Koga, arXiv:cond-mat/0603470v1.
- [47] A. Koga, N. Kawakami, T. M. Rice, and M. Sigrist, Phys. Rev. Lett. **92**, 216402 (2004).
- [48] L. de' Medici, A. Georges, S. Biermann, Phys. Rev. B **72**, 205124 (2005)

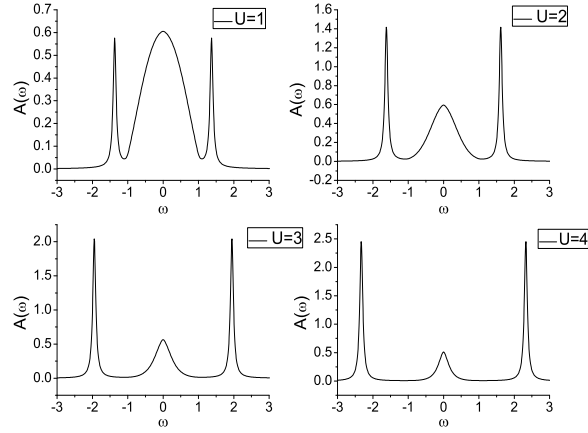


FIG. 1: The spectral function of electrons on the impurity site for an single orbital impurity model with different  $U$  and semi-circular density of states in the bath.

FIG. 2: The spectral function of electrons on the impurity site for an single orbital impurity model obtained by TMA and GA lattice with  $U = 1$ .

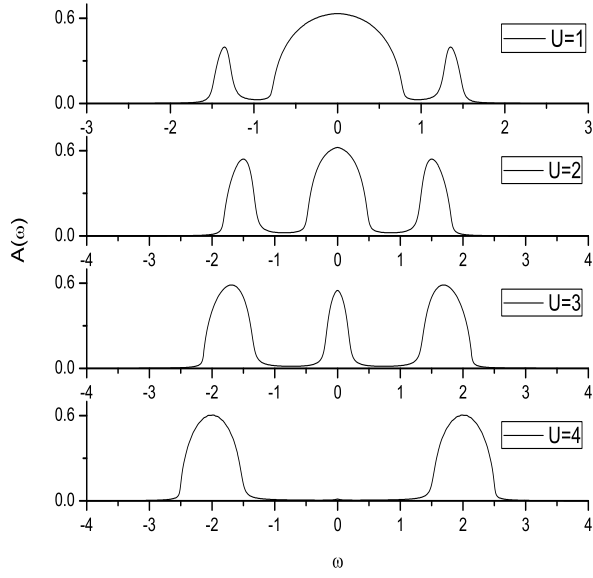


FIG. 3: The density of states (DOS) obtained by DMFT+TMA for single-band Hubbard model on Bethe lattice at half filling.

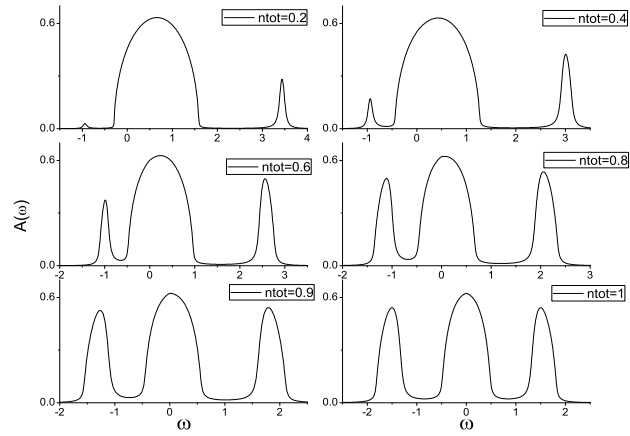


FIG. 4: The density of states (DOS) obtained by DMFT+TMA of single band Hubbard model under  $U = 2$  with different fillings.



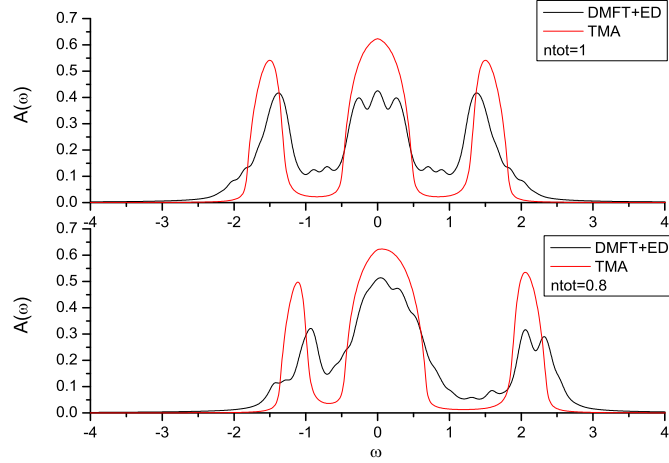


FIG. 5: Comparison of the DOS obtained by DMFT+TMA and DMFT+ED for single band Hubbard model with  $U = 2$ .

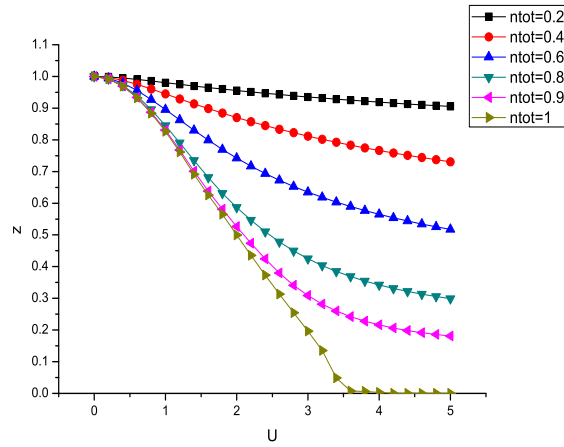


FIG. 6: Quasi-particle weight  $z$  of single band Hubbard model obtained by DMFT+TMA versus  $U$  at different fillings.

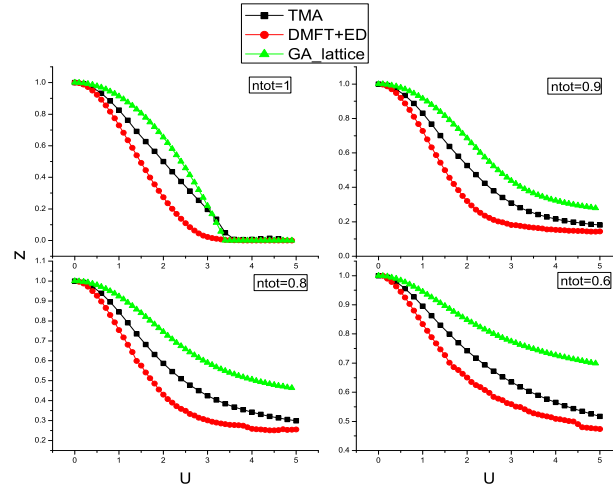


FIG. 7: Comparison of Quasi-particle weight  $z$  for the single band Hubbard model obtained by DMFT+TMA, GA lattice and DMFT+ED.

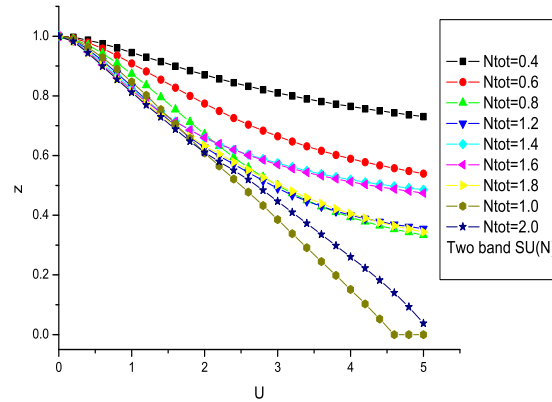


FIG. 8: Quasi-particle weight  $z$  as the function of  $U$  for the two-band Hubbard model with  $SU(N)$  symmetry obtained by DMFT+TMA.

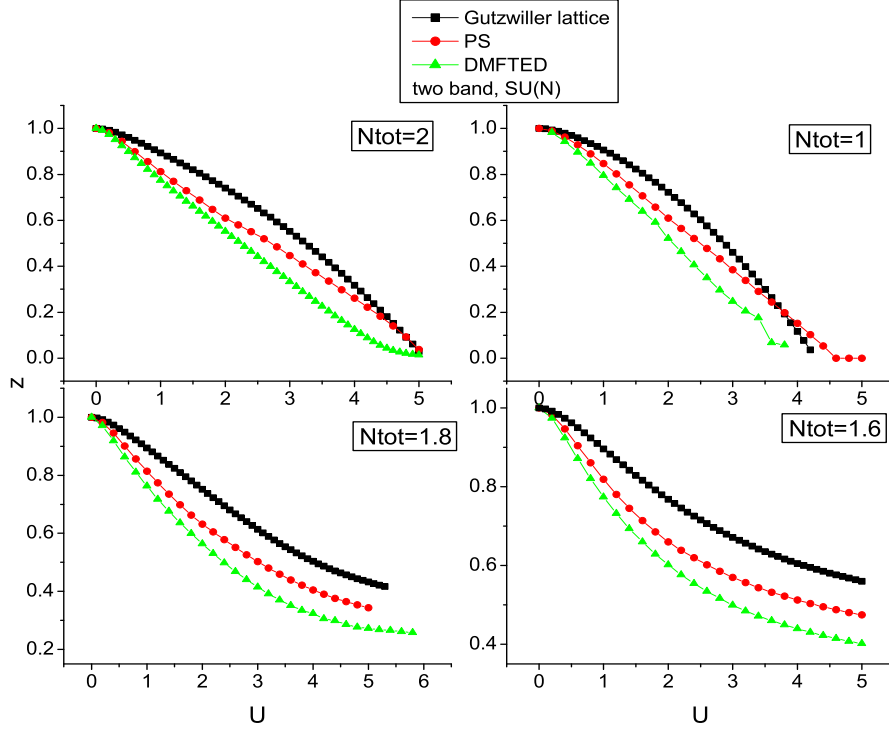


FIG. 9: Comparison of quasi-particle weight  $z$  for the two band Hubbard model with  $SU(N)$  symmetry at different fillings obtained by DMFT+TMA, GA lattice and DMFT+ED.

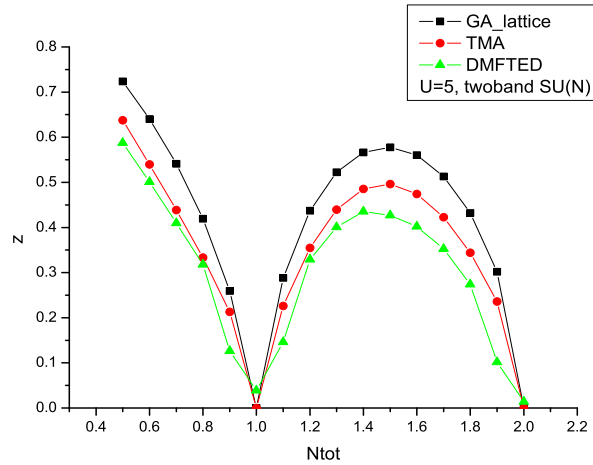


FIG. 10: Comparison of quasi-particle weight  $z$  as the function of total number of particles for the two-band Hubbard model with  $SU(N)$  symmetry at  $U = 5$  obtained by DMFT+TMA, GA lattice and DMFT+ED.

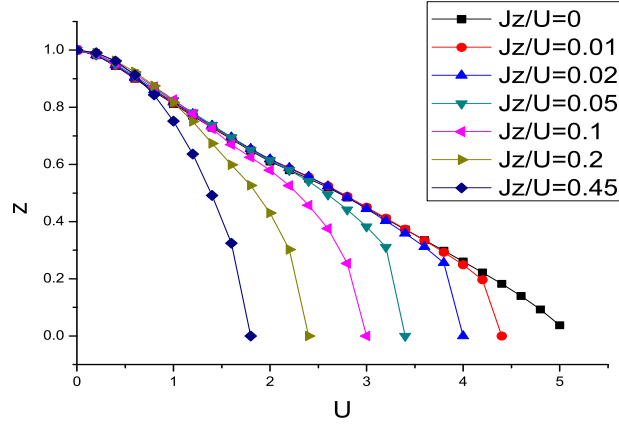


FIG. 11: Quasi-particle weight  $z$  as the function of  $U$  for the two-degenerate-band Hubbard model with longitudinal Hund's coupling  $J_z$  obtained by DMFT+TMA at different  $J_z/U$ .

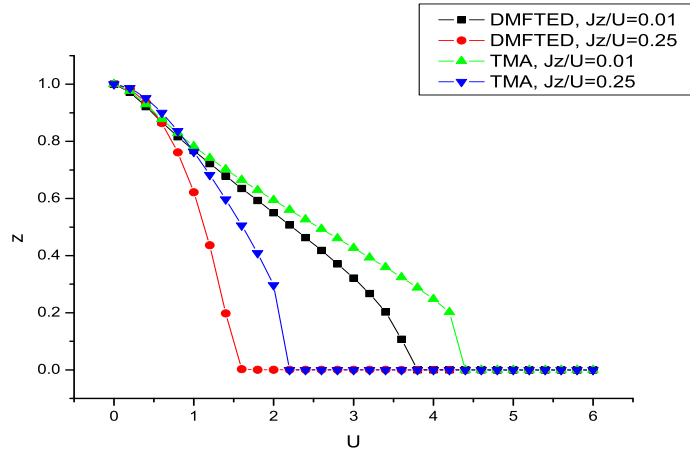


FIG. 12: Comparison of quasi-particle weight  $z$  for the two-degenerate-band Hubbard model with longitudinal Hund's coupling  $J_z$  obtained by DMFT+TMA and DMFT+ED at different  $J_z/U$ .

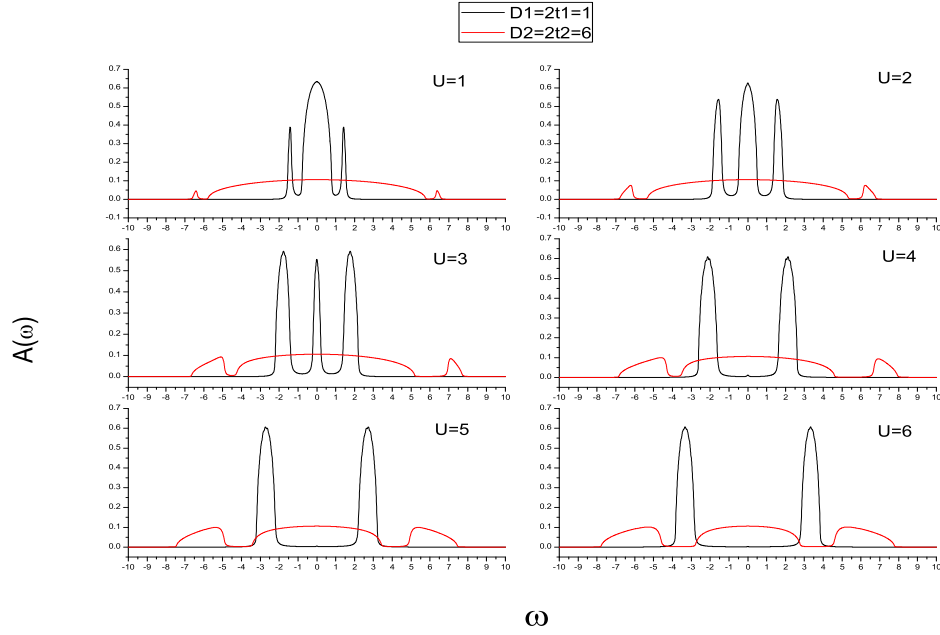


FIG. 13: The spectral functions obtained by DMFT+TMA for two-nondegenerate-band Hubbard model with band width ratio 1 : 6 under different  $U$  with  $J_z = 0.3U$ .

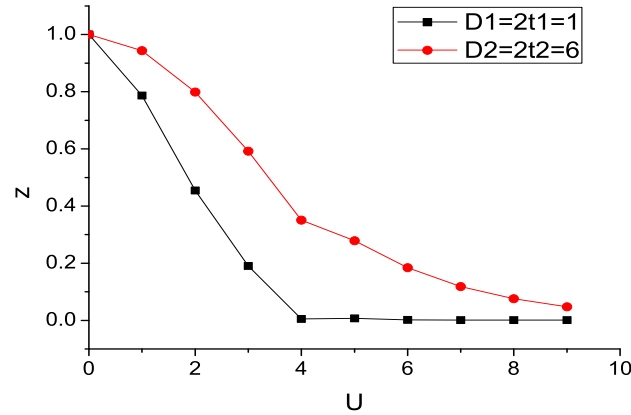


FIG. 14: Quasi-particle weight  $z$  of different bands as the function of  $U$  for two-nondegenerate-band Hubbard model with band width ratio 1 : 6 under different  $U$  with  $J_z = 0.3U$ .

# A Fast Impurity Solver Based on Gutzwiller variational approach

Jia Ning Zhuang, Lei Wang, Zhong Fang, Xi Dai

(Dated: November 6, 2018)

## Abstract

A fast impurity solver for the dynamical mean field theory(DMFT) named Two Mode Approximation (TMA) is proposed based on the Gutzwiller variational approach, which captures the main features of both the coherent and incoherent motion of the electrons. The new solver works with real frequency at zero temperature and it provides directly the spectral function of the electrons. It can be easily generalized to multi-orbital impurity problems with general on-site interactions, which makes it very useful in LDA+DMFT. Benchmarks on one and two band Hubbard models are presented, and the results agree well with those of Exact Diagonalization (ED).

PACS numbers:

## I. INTRODUCTION

The accurate calculation of the electronic structure of materials starting from first principles is a challenging problem in condensed matter science. The local density approximation (LDA) based on density functional theory (DFT) is a widely used *ab initio* method [1], which has been successfully applied to study the properties of simple metals and semiconductors as well as the band insulators. However, it can not be applied to those materials containing partially filled narrow bands from  $d$  or  $f$  shells, because of the so called strong correlation effect.

In LDA the wave like nature rather than the atomic feature of the electronic state is emphasized, so it is more suitable to describe those wide energy bands contributed by the electrons from outer shells. While for the electrons from those unclosed inner shells like  $3d$  or  $5f$  shells, some atomic features such as the multiplet structure remain, which are poorly described by LDA. Therefore for those strongly correlated materials, we have to implement LDA with some many-body techniques which can deal with the strong correlation effect and capture most of the atomic features.

One notable example of the first-principle schemes is the LDA+U method [2], which can successfully describe many interesting effects such as spin, orbital and charge ordering in transition metal compounds [3]. Although LDA+U can capture the static orbital and spin dependent physics quite well, it still can not consider the dynamical correlation effect, which causes lots of interesting phenomena like Mott transition [4] [5] [6].

Another attempt is to use Gutzwiller variational approach [7] [8] to take into account the correlation effect (LDA+G), which is superior to LDA+U and has been successfully applied to many systems[9] [10] [11]. LDA+G treatment has its advantage in describing ground state and low energy excited states, but it can not properly describe the finite temperature and dynamical properties due to the lack of high energy excited states. In order to capture the overall features of a correlated materials, more sophisticated approaches are needed.

During the past twenty years, the dynamical mean field theory (DMFT) [12] has been quickly developed to be a powerful method to solve the strongly correlated models on the lattice. DMFT maps the lattice models to the corresponding quantum impurity models subject to self-consistency conditions. Unlike the normal static mean field approaches, DMFT keeps the full local dynamics induced by the local interaction. DMFT has been successfully

applied to various of correlation problems, such as the Mott transition in Hubbard model [13] [14], the pseudo gap behavior in high  $T_c$  cuprates [15] and the heavy fermion system [16] [17]. Since DMFT can capture quite accurately the correlation feature induced by the on-site Coulomb interaction and LDA can take care of the periodic potential as well as the long range part of the Coulomb interaction, the combination of the two methods should be a very useful scheme for the first principle calculation of correlation materials. In the past twenty years, LDA+DMFT has been developed very quickly and successfully applied to many systems[18], see [19] [20] [21] and [22] for reviews of the recent developments and applications.

In LDA+DMFT, one encounters the problem of how to efficiently solve quantum impurity problems with self-consistently determined bath degrees of freedom. A fast impurity solver can be regarded as the *engine* of DMFT, which determines the efficiency and accuracy of DMFT. Many impurity solvers have been developed in the past twenty years, which can be divided into analytical methods and numerical methods. The analytical methods include equation of motion (EOM) method [23], Hubbard-I approximation [24] [25], iterative perturbation theory (IPT) [26] [27], the Non-crossing approximation(NCA) [28] and the fluctuation exchange approximation(FLEX) [29]. And the numerical methods include exact diagonalization (ED) [30], Hirsch-Fye Quantum Monte Carlo methods [31] [32] and the numerical renormalization group (NRG) [33]. Most recently a powerful continuous-time quantum Monte Carlo (CTQMC) solver [34] [35] has also been developed and applied to several realistic materials[36] [37].

All these impurity solvers have their own advantages and the limitations as well. Since most of the novel quantum phenomena in condensed matter physics happen in very low temperature, it is always very important for us to study the low temperature properties of the correlated materials using LDA+DMFT. Up to now, the impurity solvers which can work at extremely low temperature are ED, IPT and NRG. Among them, IPT can only apply to the single band system, ED and NRG are numerically quite heavy for a general multi-band system. Therefore it is very useful to develop an impurity solver working at zero temperature, which satisfies the following criteria. i) It can capture both the low energy quasi-particle physics and the high energy Hubbard bands. ii) It works with real frequency and gives the real time dynamical properties directly. iii) It is easy to be generalized to realistic multi-band systems.



Here we propose a fast impurity solver based on Gutzwiller variational approach[9] which has the above three advantages. Gutzwiller variational wave function associated with Gutzwiller approximation was first proposed to deal with lattice problems such as the Hubbard model and the periodical Anderson model[38] [39]. In the present paper, we apply a generalized Gutzwiller method called Two Mode Approximation (TMA) to calculate the Green's function for a quantum impurity model generated by DMFT. TMA is first proposed in reference[40] to calculate the spectral function for the lattice mode. Here we generalize it to the quantum impurity problem and make it a useful impurity solver for DMFT.

In TMA three different types of variational wave functions are constructed for the ground states, low energy quasi-particle states and high energy excited state respectively. All the variational parameters appearing in different wave functions are determined by minimizing the ground state energy, based on which we can obtain the electronic spectral functions over the full frequency range. The computational time is mainly determined by the minimization of the ground state energy and is similar with the previous study on lattice problem[41], which can be easily done even on a single PC. This makes the present approach a fast general solver for LDA+DMFT studies.

The paper is organized as follows. In section II we give the derivation of the method and prove that the sum rule for the electronic spectral function is satisfied. In Section III we benchmark our new impurity solver on the two-band Hubbard model with DMFT+ED. Finally a summary and the conclusions are made in section IV.

## II. DERIVATION OF THE METHOD

### A. Gutzwiller ground state

Let us first consider the following multi-orbital impurity Hamiltonian

$$\begin{aligned}
\hat{H}_{imp} &= \hat{H}_{band} + \hat{H}_{local} + \hat{H}_V \\
\hat{H}_{band} &= \sum_{k\sigma} \epsilon_{k\sigma} \hat{c}_{k\sigma}^+ \hat{c}_{k\sigma} \\
\hat{H}_{local} &= \sum_{\sigma, \sigma'} U_{\sigma\sigma'} \hat{n}_{f\sigma} \hat{n}_{f\sigma'} + \sum_{\sigma} \varepsilon_{\sigma} \hat{n}_{f\sigma} \\
\hat{H}_V &= \sum_{k\sigma} V_{k\sigma} (\hat{c}_{k\sigma}^+ \hat{f}_{\sigma} + h.c.)
\end{aligned}$$

where  $k$  denotes the energy levels in the bath and  $\sigma$  is the joint index for orbital and spin. In Gutzwiller variational approach, the ground state of the above Hamiltonian can be written as

$$|\Psi\rangle = \hat{P}|0\rangle \quad (1)$$

Where  $\hat{P}$  is the Gutzwiller projector and  $|0\rangle$  is a single Slater Determinant like wave function. Both of  $\hat{P}$  and  $|0\rangle$  will be determined by minimizing the ground state energy. Following reference [9], the Gutzwiller projector can be written in terms of the projection operators of the atomic eigen states as

$$\hat{P} = \sum_{\Gamma} \frac{\sqrt{m_{\Gamma}}}{\sqrt{m_{\Gamma}^0}} \hat{m}_{\Gamma} \quad (2)$$

In equation (2), the operator  $\hat{m}_{\Gamma} \equiv |\Gamma\rangle\langle\Gamma|$  is the projector to the eigen states  $|\Gamma\rangle$  of the atomic Hamiltonian  $\hat{H}_{local}$ , and  $m_{\Gamma}$  are the variational parameters introduced in the Gutzwiller theory. Note that if  $\hat{H}_{local}$  only contains density-density interactions, the atomic eigen states are known as the Fock states as the following[9],

$$\begin{aligned}
\Gamma \in \{ &\emptyset; (1), \dots, (2N); (1, 2), (2, 3), \dots, (2N - 1, 2N) \\
&; \dots, (1, \dots, 2N) \}
\end{aligned} \quad (3)$$

,where  $N$  is the number of orbitals.  $m_{\Gamma}^0$  is defined as

$$m_{\Gamma}^0 \equiv \langle 0 | \hat{m}_{\Gamma} | 0 \rangle \quad (4)$$

Using the operator equalities

$$\hat{m}_\Gamma = \prod_{\sigma \in \Gamma} \hat{n}_{f\sigma} \prod_{\sigma \notin \Gamma} (1 - \hat{n}_{f\sigma}) \quad (5)$$

$$\hat{n}_{f\sigma} = \sum_{\Gamma \ni \sigma} \hat{m}_\Gamma \quad (6)$$

with the definition  $n_{f\sigma}^0 \equiv \langle 0 | \hat{n}_{f\sigma} | 0 \rangle$  and  $n_{f\sigma} \equiv \langle \Psi | \hat{n}_{f\sigma} | \Psi \rangle$ , one can prove that  $m_\Gamma^0 = \prod_{\sigma \in \Gamma} n_{f\sigma}^0 \prod_{\sigma \notin \Gamma} (1 - n_{f\sigma}^0)$ ,  $n_{f\sigma}^0 = \sum_{\Gamma \ni \sigma} m_\Gamma^0$  and  $n_{f\sigma} = \sum_{\Gamma \ni \sigma} m_\Gamma$ . We would emphasize that  $n_{f\sigma}^0 = n_{f\sigma}$  for Gutzwiller type wave functions with pure density-density interaction, which greatly simplify the computation[9, 10]. Therefore the Gutzwiller ground state energy of this impurity model reads

$$E_g = \frac{\langle 0 | \hat{P} \hat{H}_{imp} \hat{P} | 0 \rangle}{\langle 0 | \hat{P}^2 | 0 \rangle} \quad (7)$$

the denominator can be expressed as

$$\langle 0 | \hat{P}^2 | 0 \rangle = \sum_{\Gamma} m_\Gamma = 1$$

while the numerator can be calculated by decomposing the projectors as in equation (5) and applying the Wick's theorem[42]. Finally we obtain the ground state energy as

$$\begin{aligned} E_g &= \sum_{k\sigma} \epsilon_{k\sigma} \langle 0 | \hat{c}_{k\sigma}^+ \hat{c}_{k\sigma} | 0 \rangle + \sum_{\Gamma} E_\Gamma m_\Gamma \\ &+ \sum_{k\sigma} z_\sigma V_{k\sigma} \langle 0 | \hat{c}_{k\sigma}^+ \hat{f}_\sigma + h.c. | 0 \rangle \end{aligned}$$

with

$$z_\sigma = \sum_{\Gamma \ni \sigma, \Gamma' = \Gamma \setminus \sigma} \frac{\sqrt{m_\Gamma m_{\Gamma'}}}{\sqrt{n_{f\sigma}^0 (1 - n_{f\sigma}^0)}}$$

The ground state wave function  $|\Psi\rangle$  can be obtained by minimizing the above energy functional respect to the  $m_\Gamma$  and non-interacting wave function  $|0\rangle$ [9, 10] along with the following constraints.

$$\sum_{\Gamma} m_\Gamma = 1 \quad (8)$$

$$n_{f\sigma} = \sum_{\Gamma \ni \sigma} m_\Gamma \quad (9)$$

## B. zero-temperature Green's function

For the impurity Hamiltonian Eq.(1), the retarded Green's function for the electrons on the impurity site reads

$$G_{\sigma}^{imp}(\omega + i\eta) = \sum_n \frac{\langle \Psi | \hat{f}_{\sigma} | n \rangle \langle n | \hat{f}_{\sigma}^{\dagger} | \Psi \rangle}{\omega + i\eta - E_n + E_g} + \sum_m \frac{\langle \Psi | \hat{f}_{\sigma}^{\dagger} | m \rangle \langle m | \hat{f}_{\sigma} | \Psi \rangle}{\omega + i\eta + E_m - E_g} \quad (10)$$

where  $|\Psi\rangle$  is the ground state of  $\hat{H}_{imp}$  with the eigen energy  $E_g$ ,  $|n\rangle$  ( $|m\rangle$ ) are the eigenstates of  $\hat{H}_{imp}$  with one more (less) electron than the ground state.  $E_n$  and  $E_m$  are the corresponding eigenvalues. The above expression is exact if the summation of  $n$  and  $m$  includes all the eigenstates. In the present paper, we apply the two mode approximation (TMA) to solve the quantum impurity problem, in which we limit the above summation in a truncated Hilbert space formed by finite number of excited states over the Gutzwiller variational ground state [40, 43]. In order to capture the basic feature of the electronic spectral function efficiently, we have to include two types of excited states in TMA, namely the quasi-particle excitations which give the right Fermi liquid behavior in low energy, and the high energy excited states which are responsible for the Hubbard bands or the atomic multiplet features. The former are called quasi-particle states and the latter are called bare-particle states in the present paper[40]. The ansatz for the excited states are the following,

$$\begin{aligned} | + k\sigma \rangle &= \hat{c}_{k\sigma}^{\dagger} \hat{P} | 0 \rangle \\ | UHB \rangle &= \hat{f}_{\sigma}^{\dagger} \hat{P} | 0 \rangle \\ | QE \rangle &= \hat{P} \hat{f}_{\sigma}^{\dagger} | 0 \rangle \\ | - k\sigma \rangle &= \hat{c}_{k\sigma} \hat{P} | 0 \rangle \\ | LHB \rangle &= \hat{f}_{\sigma} \hat{P} | 0 \rangle \\ | QH \rangle &= \hat{P} \hat{f}_{\sigma} | 0 \rangle \end{aligned}$$

where  $|QE\rangle$  ( $|QH\rangle$ ) are the quasi-particle (quasi-hole) states,  $|UHB\rangle$  ( $|LHB\rangle$ ) are the bare-particle (bare-hole) states, and  $| + -k\sigma \rangle$  represent the excitations in the bath.

The excited states listed above are neither orthogonal nor normalized, thus we have to calculate the overlaps  $\mathcal{O}_{\alpha\beta} \equiv \langle \alpha | \beta \rangle$  and the matrix elements of the Hamiltonian  $\mathcal{H}_{\alpha\beta} \equiv$

$\langle \alpha | \hat{H} | \beta \rangle$  in this truncated Hilbert space. This procedure could be easily done by applying Wick's theorem. We list all the necessary matrix elements and overlaps in the Appendix.

In order to evaluate the Green's function using expression (10), we have to first obtain the eigen states and eigen values by solving the following generalized eigen equation in the truncated Hilbert space.

$$\mathcal{H}|l\rangle = E_l \mathcal{O}|l\rangle$$

Therefore  $|l\rangle$  form a complete basis for the truncated Hilbert space and the completeness condition  $\sum_l |l\rangle \langle l| = 1$  is satisfied within the truncated Hilbert space. Since both the states  $\hat{f}_\sigma^\dagger \hat{P}|0\rangle$  and  $\hat{f}_\sigma \hat{P}|0\rangle$  are fully included in the contained Hilbert space, it is easy to prove that

$$\begin{aligned} \left(-\frac{1}{\pi}\right) \text{Im}[G_\sigma^{imp}(\omega + i\eta)] &= \langle \Psi | \hat{f}_\sigma \hat{f}_\sigma^\dagger + \hat{f}_\sigma^\dagger \hat{f}_\sigma | \Psi \rangle \\ &= 1 \end{aligned}$$

, which is the sum rule of the impurity Green's function.

### III. BENCHMARK

#### A. Impurity Spectral function

First of all we check the spectral function obtained by TMA for a single orbital impurity model with particle-hole symmetry. The density of states for the heat bath is chosen to be the semicircle with the half-width  $D = 1$ . The spectral functions for the electron on the impurity site with different Hubbard interaction  $U$  are shown in Fig.(1).

From Fig.(1) we find that the spectral function contains three parts, the quasi-particle peak and two Hubbard bands. With the increment of  $U$ , the spectral weight transfers from the low energy quasi-particle part to the Hubbard bands. And in large  $U$  limit, the distance between two Hubbard bands approaches  $U$ . All these features are consistent with the previous studies on the symmetric Anderson model [44]. In Fig.(2), we compare one spectral function for an Anderson impurity model obtained by TMA with that by the normal Gutzwiller Approximation (GA)[7, 9] for the lattice model, which only contains the quasi-particle part as

$$G_{imp}^{GWMF}(\omega + i\eta) = \frac{z^2}{\omega + i\eta + \tilde{\mu} - z^2\Delta(\omega + i\eta)} \quad (11)$$

Compared with normal Gutzwiller approximation (GA lattice), it is very clear that TMA can reproduce very nicely the low energy quasi-particle part with slightly smaller spectral weight. Therefore the current solver can be viewed as the normal Gutzwiller approximation implemented with the Hubbard bands in the high energy part of the electronic spectral functions describing the atomic features.

## B. Used as the impurity solver in DMFT

The present impurity solver can be used in the dynamical mean field theory to study the lattice models. In this paper we have studied both the single-band and two-band Hubbard model at paramagnetic phase with arbitrary fillings.

### 1. Single-band Hubbard model

We start with the single band Hubbard model on the Bethe lattice with half band width  $D = 1$ . First we check the half filling case. We show the spectral function with the increment of  $U$  in Fig.(3), from which we see that the height of quasi-particle peak changes little before Mott transition, but the integral of the quasi-particle spectrum reduces as  $U$  increases. This feature is consistent with the previous results obtained by DMFT+IPT[12].

We show the results for the systems away from half filling in Fig.(4).

With the increment of filling factor from  $N_{tot} = 0.2$  to half filling  $N_{tot} = 1.0$ , the spectral weight continuously transfers from the low energy quasi-particle part to the high energy Hubbard bands, which is consistent with the common understanding that the strong correlation effect is less pronounced when the system is doped away from half filling.

In Fig.(5), we quantitatively compare the density of states (DOS) obtained by DMFT+TMA with that by DMFT+ED. We find quite good agreement between them for both the half filling and non-half filling cases. While we also find two disagreements. Compared with the DMFT+ED results, the total spectral weight of the quasi-particle part is over-estimated while the width of the Hubbard bands is under-estimated by DMFT+TMA.

We have also calculated the quasi-particle weight  $z$ , which is a characteristic quantity describing the strength of the correlation effect and is defined as:

$$z_\sigma = \left(1 - \frac{\partial \text{Re}[\Sigma_\sigma(\omega + i\eta)]}{\partial \omega}\right)^{-1} \Big|_{\omega=0} \quad (12)$$

In Fig.(6) we show quasi-particle weight obtained by DMFT+TMA as the function of  $U$  for different filling factors. In the half filling case, the value of  $z$  decreases as the increment of  $U$  until the critical  $U_c$  for the Mott transition. As shown in Fig.(6),  $U_c$  obtained by DMFT+TMA is around 3.6, which is bigger than  $U_{c2} = 2.9$  obtained by DMFT+ED.

In Fig.(7), we compare the  $z$ -factors obtained by DMFT+TMA, Gutzwiller approximation on the lattice model (lattice GA) and DMFT+ED. As discussed in reference[10] and [40], we can only obtain the ground state energy quite accurately by lattice GA, but not for the  $z$ -factor. The reason is quite obvious that in the lattice GA only the low energy quasi-particle states in equation(10) can be considered, which limits the accuracy of  $z$ -factor. While in TMA, we first apply the DMFT scheme to treat the inter-site correlation on a mean field level, which is in principle similar with GA. Then in solving the effective impurity model, we enlarge the variational space by including more excited states, which gives us more accurate description of the low energy excited states and reduces the disagreement in  $z$ -factor with DMFT+ED results as shown in Fig.(7).

## 2. Two-band Hubbard model on the Bethe lattice

The situation becomes more complicated when we consider two-band models. We start with the simplest case that the two bands are degenerate with half bandwidth  $D_1 = D_2 = 1$  and the local part of the Hamiltonian has SU(4) symmetry, which can be written as

$$\hat{H}_{at} = U \sum_b \hat{n}_{b,\uparrow} \hat{n}_{b,\downarrow} + U \sum_{\sigma,\sigma'} \hat{n}_{1,\sigma} \hat{n}_{2,\sigma'} \quad (13)$$

We first show the quasi-particle weight obtained by DMFT+TMA versus  $U$  at different filling factors in Fig(8) and the comparison with DMFT+ED and lattice GA in Fig(9).

The Mott transition at integer fillings can be observed with  $U_c$  slightly larger than the DMFT+ED results. As shown in Fig(9), the improvement of the quasi-particle weight against the lattice GA is quite dramatic, which indicates that even for the low energy quasi-particle part the DMFT+TMA is better than applying the GA directly to the lattice model.

The behavior of  $z$  as the function of the filling factor for fixed  $U = 5.0$  is shown in Fig(10), from which we can find that compared with lattice GA the results obtained by DMFT+TMA is much closer to DMFT+ED.

Next we take the Hund's coupling constant  $J$  into account. Then the atomic Hamiltonian becomes

$$\begin{aligned} \hat{H}_{at} = & U \sum_b \hat{n}_{b,\uparrow} \hat{n}_{b,\downarrow} + U' \sum_{\sigma,\sigma'} \hat{n}_{1,\sigma} \hat{n}_{2,\sigma'} - J \sum_{\sigma} \hat{n}_{1,\sigma} \hat{n}_{2,\sigma} \\ & + J \sum_{\sigma} \hat{c}_{1,\sigma}^+ \hat{c}_{2,-\sigma}^+ \hat{c}_{1,-\sigma} \hat{c}_{2,\sigma} + J(\hat{c}_{1,\uparrow}^+ \hat{c}_{1,\downarrow}^+ \hat{c}_{2,\downarrow} \hat{c}_{2,\uparrow} \\ & + \hat{c}_{2,\uparrow}^+ \hat{c}_{2,\downarrow}^+ \hat{c}_{1,\downarrow} \hat{c}_{1,\uparrow}) \end{aligned} \quad (14)$$

We have the relation  $U - U' = 2J$  for system with cubic symmetry[45]. In the current study, we only keep the longitudinal part of the Hund's rule coupling and neglect the spin flip and pair hopping terms which correspond to the last two terms in the above equation. The results for the full rotational invariance interaction will be studied in detail and published elsewhere.

The quasi-particle weight obtained by DMFT+TMA as the function of  $U$  is shown in Fig.(11). We also compare the results with DMFT+ED in Fig.(12), from which we find that  $U_c$  obtained from TMA is larger than that of DMFT+ED as for the single band model.

In Fig.(11), we find that the Brinkman-Rice(BR) transition is continuous *only* at the point  $J_z = 0$  and first order like for all non-zero  $J_z$ , which is similar with the results in reference [9] obtained by rotational invariant Gutzwiller approximation. This similarity indicates that for degenerate multi-band Hubbard model the basic feature of the BR transition does not strongly relies on the variational invariant treatment of the interaction. Moreover, the similar discontinuity and the tendency that the critical  $U_c$  decreases as  $J_z/U$  increases is also obtained in [46], where the self-energy functional method is used.

However, for the non-degenerate multi-band models, i.e. the two-band model with different band widths, the correct variational invariant treatment is necessary to obtain some of the qualitative features like the orbital selective Mott transition (OSMT)[47]. The detailed study for the OSMT using the variational invariant TMA solver will be presented elsewhere. Here we only give the results for an extreme case, where the band width difference of the two bands is very large. In Fig.(13) and (14), we represent the DOS as well as the quasi-particle weight as the functional of  $U$  with fixed  $J_z/U = 0.3$  and half band width  $D_1 = 1.0$ ,  $D_2 = 6.0$ .



Obviously in such extreme case, the system is in the orbital selective Mott phase which is consistent with reference [48].

#### IV. CONCLUSIONS

In this paper we present a new impurity solver named Two Mode Approximation (TMA) for the multi-orbital quantum impurity model generated by DMFT. By constructing the trial wave functions based on the Gutzwiller variational theory not only for the ground state but also the low energy and high energy excited states, we can obtain the spectral functions of the electrons on the impurity level with the satisfactory of the sum rule. Compared with other popular impurity solvers, TMA works with the real frequency and can obtain both the low energy quasi-particle and high energy Hubbard band behavior. Moreover TMA can be generalized to treat the problem with quite general on-site interaction, which make it a good solver to be used in LDA+DMFT.

ACKNOWLEDGEMENT: The authors would thank Q. M. Liu, X. Y. Deng, Y. Wan and N.H. Tong for their helpful discussions. We acknowledge the supports from NSF of China , and that from the 973 program of China (No.2007CB925000).

#### V. APPENDIX: OVERLAPS AND HAMILTONIAN ELEMENTS

##### A. Overlaps

Define

$$z_\sigma = \sum_{\Gamma \ni \sigma, \Gamma' = \Gamma \setminus \sigma} \frac{\sqrt{m_\Gamma m_{\Gamma'}}}{\sqrt{n_{f\sigma}^0 (1 - n_{f\sigma}^0)}}$$

the non-vanishing overlaps are

$$\langle +k_1\sigma | +k_2\sigma \rangle = \langle 0 | \hat{c}_{k_1\sigma} \hat{c}_{k_2\sigma}^+ | 0 \rangle$$

$$\langle +k\sigma | UHB \rangle = z_\sigma \langle 0 | \hat{c}_{k\sigma} \hat{f}_\sigma^\dagger | 0 \rangle$$

$$\langle +k\sigma | QE \rangle = \langle 0 | \hat{c}_{k\sigma} \hat{f}_\sigma^\dagger | 0 \rangle$$

$$\langle UHB|UHB\rangle = (1 - n_{f\sigma}^0)$$

$$\langle UHB|QE\rangle = z_\sigma(1 - n_{f\sigma}^0)$$

$$\langle QE|QE\rangle = (1 - n_{f\sigma}^0)$$

$$\langle -k_1\sigma | -k_2\sigma\rangle = \langle 0|\hat{c}_{k_1\sigma}^+\hat{c}_{k_2\sigma}|0\rangle$$

$$\langle -k\sigma |LHB\rangle = z_\sigma\langle 0|\hat{c}_{k\sigma}^+\hat{f}_\sigma|0\rangle$$

$$\langle -k\sigma |QH\rangle = \langle 0|\hat{c}_{k\sigma}^+\hat{f}_\sigma|0\rangle$$

$$\langle LHB|LHB\rangle = n_{f\sigma}^0$$

$$\langle LHB|QH\rangle = z_\sigma n_{f\sigma}^0$$

$$\langle LHB|LHB\rangle = n_{f\sigma}^0$$

## B. Hamiltonian Elements

$$\begin{aligned}\hat{H} &= \hat{H}_{band} + \hat{H}_{local} + \hat{H}_V \\ \hat{H}_{band} &= \sum_{k\sigma} \epsilon_{k\sigma} \hat{c}_{k\sigma}^+ \hat{c}_{k\sigma} \\ \hat{H}_{local} &= \sum_{\Gamma} E_{\Gamma} \hat{m}_{\Gamma} + \sum_{\sigma} \varepsilon_{\sigma} \sum_{\Gamma \ni \sigma} \hat{m}_{\Gamma} \\ \hat{H}_V &= \sum_{k\sigma} V_{k\sigma} (\hat{c}_{k\sigma}^+ \hat{f}_{\sigma} + h.c.)\end{aligned}$$

1. *H*-band

Define

$$\begin{aligned}
x_{\sigma\sigma'} &= \sum_{\substack{\Gamma_2 \ni \sigma, \Gamma_2 \ni \sigma' \\ \Gamma_1 = \Gamma_2 \setminus \sigma'}} \frac{\sqrt{m_{\Gamma_1} m_{\Gamma_2}}}{n_{f\sigma}^0 \sqrt{n_{f\sigma'}^0 (1 - n_{f\sigma'}^0)}} \\
y_{\sigma\sigma'} &= \sum_{\substack{\Gamma_1 \ni \sigma, \Gamma_1 \ni \sigma' \\ \Gamma_2 = \Gamma_1 \cup \sigma' \setminus \sigma}} \frac{\sqrt{m_{\Gamma_1} m_{\Gamma_2}}}{\sqrt{n_{f\sigma}^0 (1 - n_{f\sigma}^0) n_{f\sigma'}^0 (1 - n_{f\sigma'}^0)}} \\
w_{\sigma\sigma'} &= \sum_{\substack{\Gamma_2 \ni \sigma, \Gamma_2 \ni \sigma' \\ \Gamma_1 = \Gamma_2 \cup \sigma \cup \sigma'}} \frac{\sqrt{m_{\Gamma_1} m_{\Gamma_2}}}{\sqrt{n_{f\sigma}^0 (1 - n_{f\sigma}^0) n_{f\sigma'}^0 (1 - n_{f\sigma'}^0)}} \\
v_{\sigma\sigma'} &= \sum_{\substack{\Gamma_1 \ni \sigma, \Gamma_1 \ni \sigma' \\ \Gamma_2 = \Gamma_1 \cup \sigma'}} \frac{\sqrt{m_{\Gamma_1} m_{\Gamma_2}}}{(1 - n_{f\sigma}^0) \sqrt{n_{f\sigma'}^0 (1 - n_{f\sigma'}^0)}}
\end{aligned}$$

and

$$\begin{aligned}
B_{\sigma\sigma'}^{++} &= \sum_{\Gamma \ni \sigma, \Gamma \ni \sigma'} \frac{m_{\Gamma}}{n_{f\sigma}^0 n_{f\sigma'}^0} \\
B_{\sigma\sigma'}^{+-} &= \sum_{\Gamma \ni \sigma, \Gamma \ni \sigma'} \frac{m_{\Gamma}}{n_{f\sigma}^0 (1 - n_{f\sigma'}^0)} \\
B_{\sigma\sigma'}^{--} &= \sum_{\Gamma \ni \sigma, \Gamma \ni \sigma'} \frac{m_{\Gamma}}{(1 - n_{f\sigma}^0) (1 - n_{f\sigma'}^0)}
\end{aligned}$$

we will have

$$\begin{aligned}
\langle +k_1\sigma \mid \hat{H}_{band} \mid +k_2\sigma \rangle &= \sum_{k'\sigma'} \epsilon_{k'\sigma'} [\delta_{\sigma\sigma'} \langle 0 \mid \hat{c}_{k_1\sigma} \hat{c}_{k'\sigma}^+ \hat{c}_{k'\sigma} \hat{c}_{k_2\sigma}^+ \mid 0 \rangle \\
&\quad + (1 - \delta_{\sigma\sigma'}) \\
&\quad \times (B_{\sigma\sigma'}^{++} \langle 0 \mid \hat{c}_{k_1\sigma} \hat{c}_{k_2\sigma}^+ \hat{f}_{\sigma}^{\dagger} \hat{f}_{\sigma} \mid 0 \rangle \langle 0 \mid \hat{c}_{k'\sigma'}^+ \hat{c}_{k'\sigma'} \hat{f}_{\sigma'}^{\dagger} \hat{f}_{\sigma'} \mid 0 \rangle \\
&\quad + B_{\sigma\sigma'}^{+-} \langle 0 \mid \hat{c}_{k_1\sigma} \hat{c}_{k_2\sigma}^+ \hat{f}_{\sigma}^{\dagger} \hat{f}_{\sigma} \mid 0 \rangle \langle 0 \mid \hat{c}_{k'\sigma'}^+ \hat{c}_{k'\sigma'} \hat{f}_{\sigma'}^{\dagger} \hat{f}_{\sigma'} \mid 0 \rangle \\
&\quad + B_{\sigma'\sigma}^{+-} \langle 0 \mid \hat{c}_{k_1\sigma} \hat{c}_{k_2\sigma}^+ \hat{f}_{\sigma} \hat{f}_{\sigma}^{\dagger} \mid 0 \rangle \langle 0 \mid \hat{c}_{k'\sigma'}^+ \hat{c}_{k'\sigma'} \hat{f}_{\sigma'}^{\dagger} \hat{f}_{\sigma'} \mid 0 \rangle \\
&\quad + B_{\sigma\sigma'}^{--} \langle 0 \mid \hat{c}_{k_1\sigma} \hat{c}_{k_2\sigma}^+ \hat{f}_{\sigma} \hat{f}_{\sigma}^{\dagger} \mid 0 \rangle \langle 0 \mid \hat{c}_{k'\sigma'}^+ \hat{c}_{k'\sigma'} \hat{f}_{\sigma'}^{\dagger} \hat{f}_{\sigma'} \mid 0 \rangle)
\end{aligned}$$

$$\begin{aligned} \langle +k\sigma | \hat{H}_{band} | UHB \rangle &= \sum_{k'\sigma'} \epsilon_{k'\sigma'} [\delta_{\sigma\sigma'} z_\sigma \langle 0 | \hat{c}_{k\sigma} \hat{c}_{k'\sigma}^+ \hat{c}_{k'\sigma} \hat{f}_\sigma^\dagger | 0 \rangle \\ &\quad + (1 - \delta_{\sigma\sigma'}) \langle 0 | \hat{c}_{k\sigma} \hat{f}_\sigma^\dagger | 0 \rangle (x_{\sigma'\sigma} \langle 0 | \hat{c}_{k'\sigma}^+ \hat{c}_{k'\sigma'} \hat{f}_{\sigma'}^\dagger \hat{f}_{\sigma'} | 0 \rangle + v_{\sigma'\sigma} \langle 0 | \hat{c}_{k'\sigma}^+ \hat{c}_{k'\sigma'} \hat{f}_{\sigma'} \hat{f}_{\sigma'}^\dagger | 0 \rangle)] \end{aligned}$$

$$\begin{aligned} \langle +k\sigma | \hat{H}_{band} | QE \rangle &= \sum_{k'\sigma'} \epsilon_{k'\sigma'} [\delta_{\sigma\sigma'} \langle 0 | \hat{c}_{k\sigma} \hat{c}_{k'\sigma}^+ \hat{c}_{k'\sigma} \hat{f}_\sigma^\dagger | 0 \rangle \\ &\quad + (1 - \delta_{\sigma\sigma'}) \langle 0 | \hat{c}_{k\sigma} \hat{f}_\sigma^\dagger | 0 \rangle (B_{\sigma\sigma'}^{++} \langle 0 | \hat{c}_{k'\sigma}^+ \hat{c}_{k'\sigma'} \hat{f}_{\sigma'}^\dagger \hat{f}_{\sigma'} | 0 \rangle + B_{\sigma\sigma'}^{+-} \langle 0 | \hat{c}_{k'\sigma}^+ \hat{c}_{k'\sigma'} \hat{f}_{\sigma'} \hat{f}_{\sigma'}^\dagger | 0 \rangle)] \end{aligned}$$

$$\begin{aligned} \langle UHB | \hat{H}_{band} | UHB \rangle &= \sum_{k'\sigma'} \epsilon_{k'\sigma'} [\delta_{\sigma\sigma'} \langle 0 | \hat{f}_\sigma \hat{c}_{k'\sigma}^+ \hat{c}_{k'\sigma} \hat{f}_\sigma^\dagger | 0 \rangle \\ &\quad + (1 - \delta_{\sigma\sigma'}) (1 - n_{f\sigma}^0) \\ &\quad \times (B_{\sigma\sigma'}^{+-} \langle 0 | \hat{c}_{k'\sigma}^+ \hat{c}_{k'\sigma'} \hat{f}_{\sigma'}^\dagger \hat{f}_{\sigma'} | 0 \rangle + B_{\sigma\sigma'}^{--} \langle 0 | \hat{c}_{k'\sigma}^+ \hat{c}_{k'\sigma'} \hat{f}_{\sigma'} \hat{f}_{\sigma'}^\dagger | 0 \rangle)] \end{aligned}$$

$$\begin{aligned} \langle UHB | \hat{H}_{band} | QE \rangle &= \sum_{k'\sigma'} \epsilon_{k'\sigma'} [\delta_{\sigma\sigma'} z_\sigma \langle 0 | \hat{f}_\sigma \hat{c}_{k'\sigma}^+ \hat{c}_{k'\sigma} \hat{f}_\sigma^\dagger | 0 \rangle \\ &\quad + (1 - \delta_{\sigma\sigma'}) (1 - n_{f\sigma}^0) \\ &\quad \times (x_{\sigma'\sigma} \langle 0 | \hat{c}_{k'\sigma}^+ \hat{c}_{k'\sigma'} \hat{f}_{\sigma'}^\dagger \hat{f}_{\sigma'} | 0 \rangle + v_{\sigma'\sigma} \langle 0 | \hat{c}_{k'\sigma}^+ \hat{c}_{k'\sigma'} \hat{f}_{\sigma'} \hat{f}_{\sigma'}^\dagger | 0 \rangle)] \end{aligned}$$

$$\begin{aligned} \langle QE | \hat{H}_{band} | QE \rangle &= \sum_{k'\sigma'} \epsilon_{k'\sigma'} [\delta_{\sigma\sigma'} \langle 0 | \hat{f}_\sigma \hat{c}_{k'\sigma}^+ \hat{c}_{k'\sigma} \hat{f}_\sigma^\dagger | 0 \rangle \\ &\quad + (1 - \delta_{\sigma\sigma'}) (1 - n_{f\sigma}^0) \\ &\quad \times (B_{\sigma\sigma'}^{++} \langle 0 | \hat{c}_{k'\sigma}^+ \hat{c}_{k'\sigma'} \hat{f}_{\sigma'}^\dagger \hat{f}_{\sigma'} | 0 \rangle + B_{\sigma\sigma'}^{+-} \langle 0 | \hat{c}_{k'\sigma}^+ \hat{c}_{k'\sigma'} \hat{f}_{\sigma'} \hat{f}_{\sigma'}^\dagger | 0 \rangle)] \end{aligned}$$

$$\begin{aligned} \langle -k_1\sigma | \hat{H}_{band} | -k_2\sigma \rangle &= \sum_{k'\sigma'} \epsilon_{k'\sigma'} [\delta_{\sigma\sigma'} \langle 0 | \hat{c}_{k_1\sigma}^+ \hat{c}_{k'\sigma}^+ \hat{c}_{k'\sigma} \hat{c}_{k_2\sigma} | 0 \rangle \\ &\quad + (1 - \delta_{\sigma\sigma'}) \\ &\quad \times (B_{\sigma\sigma'}^{++} \langle 0 | \hat{c}_{k_1\sigma}^+ \hat{c}_{k_2\sigma} \hat{f}_\sigma^\dagger \hat{f}_\sigma | 0 \rangle \langle 0 | \hat{c}_{k'\sigma}^+ \hat{c}_{k'\sigma'} \hat{f}_{\sigma'}^\dagger \hat{f}_{\sigma'} | 0 \rangle \\ &\quad + B_{\sigma\sigma'}^{+-} \langle 0 | \hat{c}_{k_1\sigma}^+ \hat{c}_{k_2\sigma} \hat{f}_\sigma^\dagger \hat{f}_\sigma | 0 \rangle \langle 0 | \hat{c}_{k'\sigma}^+ \hat{c}_{k'\sigma'} \hat{f}_{\sigma'} \hat{f}_{\sigma'}^\dagger | 0 \rangle \\ &\quad + B_{\sigma\sigma'}^{-+} \langle 0 | \hat{c}_{k_1\sigma}^+ \hat{c}_{k_2\sigma} \hat{f}_\sigma \hat{f}_\sigma^\dagger | 0 \rangle \langle 0 | \hat{c}_{k'\sigma}^+ \hat{c}_{k'\sigma'} \hat{f}_{\sigma'}^\dagger \hat{f}_{\sigma'} | 0 \rangle \\ &\quad + B_{\sigma\sigma'}^{--} \langle 0 | \hat{c}_{k_1\sigma}^+ \hat{c}_{k_2\sigma} \hat{f}_\sigma \hat{f}_\sigma^\dagger | 0 \rangle \langle 0 | \hat{c}_{k'\sigma}^+ \hat{c}_{k'\sigma'} \hat{f}_{\sigma'} \hat{f}_{\sigma'}^\dagger | 0 \rangle)] \end{aligned}$$

$$\begin{aligned} \langle -k\sigma | \hat{H}_{band} | LHB \rangle &= \sum_{k'\sigma'} \epsilon_{k'\sigma'} (\delta_{\sigma\sigma'} z_\sigma \langle 0 | \hat{c}_{k\sigma}^+ \hat{c}_{k'\sigma}^+ \hat{c}_{k'\sigma} \hat{f}_\sigma | 0 \rangle \\ &\quad + (1 - \delta_{\sigma\sigma'}) \langle 0 | \hat{c}_{k\sigma}^+ \hat{f}_\sigma | 0 \rangle (x_{\sigma'\sigma} \langle 0 | \hat{c}_{k'\sigma'}^+ \hat{c}_{k'\sigma'} \hat{f}_{\sigma'}^\dagger \hat{f}_{\sigma'} | 0 \rangle + v_{\sigma'\sigma} \langle 0 | \hat{c}_{k'\sigma'}^+ \hat{c}_{k'\sigma'} \hat{f}_{\sigma'} \hat{f}_{\sigma'}^\dagger | 0 \rangle)) \end{aligned}$$

$$\begin{aligned} \langle -k\sigma | \hat{H}_{band} | QH \rangle &= \sum_{k'\sigma'} \epsilon_{k'\sigma'} (\delta_{\sigma\sigma'} \langle 0 | \hat{c}_{k\sigma}^+ \hat{c}_{k'\sigma}^+ \hat{c}_{k'\sigma} \hat{f}_\sigma | 0 \rangle \\ &\quad + (1 - \delta_{\sigma\sigma'}) \langle 0 | \hat{c}_{k\sigma}^+ \hat{f}_\sigma | 0 \rangle (B_{\sigma\sigma'}^{-+} \langle 0 | \hat{c}_{k'\sigma'}^+ \hat{c}_{k'\sigma'} \hat{f}_{\sigma'}^\dagger \hat{f}_{\sigma'} | 0 \rangle + B_{\sigma\sigma'}^{--} \langle 0 | \hat{c}_{k'\sigma'}^+ \hat{c}_{k'\sigma'} \hat{f}_{\sigma'} \hat{f}_{\sigma'}^\dagger | 0 \rangle)) \end{aligned}$$

$$\begin{aligned} \langle LHB | \hat{H}_{band} | LHB \rangle &= \sum_{k'\sigma'} \epsilon_{k'\sigma'} [\delta_{\sigma\sigma'} \langle 0 | \hat{f}_\sigma^\dagger \hat{c}_{k'\sigma}^+ \hat{c}_{k'\sigma} \hat{f}_\sigma | 0 \rangle \\ &\quad + (1 - \delta_{\sigma\sigma'}) n_{f_\sigma}^0 \\ &\quad \times (B_{\sigma\sigma'}^{++} \langle 0 | \hat{c}_{k'\sigma'}^+ \hat{c}_{k'\sigma'} \hat{f}_{\sigma'}^\dagger \hat{f}_{\sigma'} | 0 \rangle + B_{\sigma\sigma'}^{+-} \langle 0 | \hat{c}_{k'\sigma'}^+ \hat{c}_{k'\sigma'} \hat{f}_{\sigma'} \hat{f}_{\sigma'}^\dagger | 0 \rangle)] \end{aligned}$$

$$\begin{aligned} \langle LHB | \hat{H}_{band} | QH \rangle &= \sum_{k'\sigma'} \epsilon_{k'\sigma'} [\delta_{\sigma\sigma'} z_\sigma \langle 0 | \hat{f}_\sigma^\dagger \hat{c}_{k'\sigma}^+ \hat{c}_{k'\sigma} \hat{f}_\sigma | 0 \rangle \\ &\quad + (1 - \delta_{\sigma\sigma'}) n_{f_\sigma}^0 \\ &\quad \times (x_{\sigma'\sigma} \langle 0 | \hat{c}_{k'\sigma'}^+ \hat{c}_{k'\sigma'} \hat{f}_{\sigma'}^\dagger \hat{f}_{\sigma'} | 0 \rangle + v_{\sigma'\sigma} \langle 0 | \hat{c}_{k'\sigma'}^+ \hat{c}_{k'\sigma'} \hat{f}_{\sigma'} \hat{f}_{\sigma'}^\dagger | 0 \rangle)] \end{aligned}$$

$$\begin{aligned} \langle QH | \hat{H}_{band} | QH \rangle &= \sum_{k'\sigma'} \epsilon_{k'\sigma'} [\delta_{\sigma\sigma'} \langle 0 | \hat{f}_\sigma^\dagger \hat{c}_{k'\sigma}^+ \hat{c}_{k'\sigma} \hat{f}_\sigma | 0 \rangle \\ &\quad + (1 - \delta_{\sigma\sigma'}) n_{f_\sigma}^0 \\ &\quad \times (B_{\sigma\sigma'}^{-+} \langle 0 | \hat{c}_{k'\sigma'}^+ \hat{c}_{k'\sigma'} \hat{f}_{\sigma'}^\dagger \hat{f}_{\sigma'} | 0 \rangle + B_{\sigma\sigma'}^{--} \langle 0 | \hat{c}_{k'\sigma'}^+ \hat{c}_{k'\sigma'} \hat{f}_{\sigma'} \hat{f}_{\sigma'}^\dagger | 0 \rangle)] \end{aligned}$$

## 2. $H_{local}$

Here we define a function for set:

$$A_{\sigma,\Gamma} = \begin{cases} 1, & \text{if } \sigma \in \Gamma \\ 0, & \text{if } \sigma \notin \Gamma \end{cases}$$

then define

$$S_\Gamma = E_\Gamma + \sum_{\sigma'} \varepsilon_{\sigma'} A_{\sigma', \Gamma}$$

and

$$\begin{aligned} S_1 &= \sum_{\Gamma} E_\Gamma m_\Gamma + \sum_{\sigma'} \varepsilon_{\sigma'} \sum_{\Gamma \ni \sigma'} m_\Gamma \\ &= \sum_{\Gamma} m_\Gamma S_\Gamma \end{aligned}$$

$$\begin{aligned} S_2(\sigma) &= \sum_{\Gamma} E_\Gamma A_{\sigma, \Gamma} \sqrt{m_\Gamma m_{\Gamma \setminus \sigma}} + \sum_{\sigma'} \varepsilon_{\sigma'} \sum_{\Gamma \ni \sigma'} A_{\sigma, \Gamma} \sqrt{m_\Gamma m_{\Gamma \setminus \sigma}} \\ &= \sum_{\Gamma} A_{\sigma, \Gamma} \sqrt{m_\Gamma m_{\Gamma \setminus \sigma}} S_\Gamma \end{aligned}$$

$$\begin{aligned} S_3(\sigma) &= \sum_{\Gamma} E_\Gamma A_{\sigma, \Gamma} m_\Gamma + \sum_{\sigma'} \varepsilon_{\sigma'} \sum_{\Gamma \ni \sigma'} A_{\sigma, \Gamma} m_\Gamma \\ &= \sum_{\Gamma} A_{\sigma, \Gamma} m_\Gamma S_\Gamma \end{aligned}$$

$$\begin{aligned} S_4(\sigma) &= \sum_{\Gamma} E_\Gamma A_{\sigma, \Gamma} m_{\Gamma \setminus \sigma} + \sum_{\sigma'} \varepsilon_{\sigma'} \sum_{\Gamma \ni \sigma'} A_{\sigma, \Gamma} m_{\Gamma \setminus \sigma} \\ &= \sum_{\Gamma} A_{\sigma, \Gamma} m_{\Gamma \setminus \sigma} S_\Gamma \end{aligned}$$

$$\begin{aligned} S_5(\sigma) &= \sum_{\Gamma} E_\Gamma (1 - A_{\sigma, \Gamma}) \sqrt{m_\Gamma m_{\Gamma \cup \sigma}} + \sum_{\sigma'} \varepsilon_{\sigma'} \sum_{\Gamma \ni \sigma'} (1 - A_{\sigma, \Gamma}) \sqrt{m_\Gamma m_{\Gamma \cup \sigma}} \\ &= \sum_{\Gamma} (1 - A_{\sigma, \Gamma}) \sqrt{m_\Gamma m_{\Gamma \cup \sigma}} S_\Gamma \end{aligned}$$

$$\begin{aligned} S_6(\sigma) &= \sum_{\Gamma} E_\Gamma (1 - A_{\sigma, \Gamma}) m_\Gamma + \sum_{\sigma'} \varepsilon_{\sigma'} \sum_{\Gamma \ni \sigma'} (1 - A_{\sigma, \Gamma}) m_\Gamma \\ &= \sum_{\Gamma} (1 - A_{\sigma, \Gamma}) m_\Gamma S_\Gamma \end{aligned}$$

$$\begin{aligned} S_7(\sigma) &= \sum_{\Gamma} E_\Gamma (1 - A_{\sigma, \Gamma}) m_{\Gamma \cup \sigma} + \sum_{\sigma'} \varepsilon_{\sigma'} \sum_{\Gamma \ni \sigma'} (1 - A_{\sigma, \Gamma}) m_{\Gamma \cup \sigma} \\ &= \sum_{\Gamma} (1 - A_{\sigma, \Gamma}) m_{\Gamma \cup \sigma} S_\Gamma \end{aligned}$$

$$\begin{aligned}
S_{25}(\sigma) &= \sum_{\Gamma} E_{\Gamma} \left[ A_{\sigma, \Gamma} \frac{m_{\Gamma}}{n_{f\sigma}^0} - (1 - A_{\sigma, \Gamma}) \frac{m_{\Gamma}}{1 - n_{f\sigma}^0} \right] \\
&\quad + \sum_{\sigma'} \varepsilon_{\sigma'} \sum_{\Gamma \ni \sigma'} A_{\sigma', \Gamma} \left[ A_{\sigma, \Gamma} \frac{m_{\Gamma}}{n_{f\sigma}^0} - (1 - A_{\sigma, \Gamma}) \frac{m_{\Gamma}}{1 - n_{f\sigma}^0} \right] \\
&= \left[ A_{\sigma, \Gamma} \frac{m_{\Gamma}}{n_{f\sigma}^0} - (1 - A_{\sigma, \Gamma}) \frac{m_{\Gamma}}{1 - n_{f\sigma}^0} \right] S_{\Gamma}
\end{aligned}$$

thus

$$\langle +k_1\sigma \mid \hat{H}_{local} \mid +k_2\sigma \rangle = \langle 0 \mid \hat{c}_{k_1\sigma} \hat{c}_{k_2\sigma}^+ \mid 0 \rangle S_1 + \langle 0 \mid \hat{c}_{k_1\sigma} \hat{f}_{\sigma}^{\dagger} \mid 0 \rangle \langle 0 \mid \hat{f}_{\sigma} \hat{c}_{k_2\sigma}^+ \mid 0 \rangle S_{25}(\sigma)$$

$$\langle +k\sigma \mid \hat{H}_{local} \mid UHB \rangle = \frac{1}{\sqrt{n_{f\sigma}^0(1 - n_{f\sigma}^0)}} \langle 0 \mid \hat{c}_{k\sigma} \hat{f}_{\sigma}^{\dagger} \mid 0 \rangle S_2(\sigma)$$

$$\langle +k\sigma \mid \hat{H}_{local} \mid QE \rangle = \frac{1}{n_{f\sigma}^0} \langle 0 \mid \hat{c}_{k\sigma} \hat{f}_{\sigma}^{\dagger} \mid 0 \rangle S_3(\sigma)$$

$$\langle UHB \mid \hat{H}_{local} \mid UHB \rangle = S_4(\sigma)$$

$$\langle UHB \mid \hat{H}_{local} \mid QE \rangle = \frac{\sqrt{1 - n_{f\sigma}^0}}{\sqrt{n_{f\sigma}^0}} S_2(\sigma)$$

$$\langle QE \mid \hat{H}_{local} \mid QE \rangle = \frac{1 - n_{f\sigma}^0}{n_{f\sigma}^0} S_3(\sigma)$$

$$\langle -k_1\sigma \mid \hat{H}_{local} \mid -k_2\sigma \rangle = \langle 0 \mid \hat{c}_{k_1\sigma}^+ \hat{c}_{k_2\sigma} \mid 0 \rangle S_1 - \langle 0 \mid \hat{c}_{k_1\sigma}^+ \hat{f}_{\sigma} \mid 0 \rangle \langle 0 \mid \hat{f}_{\sigma} \hat{c}_{k_2\sigma} \mid 0 \rangle S_{25}(\sigma)$$

$$\langle -k\sigma \mid \hat{H}_{local} \mid LHB \rangle = \frac{1}{\sqrt{n_{f\sigma}^0(1 - n_{f\sigma}^0)}} \langle 0 \mid \hat{c}_{k\sigma}^+ \hat{f}_{\sigma} \mid 0 \rangle S_5(\sigma)$$

$$\langle -k\sigma \mid \hat{H}_{local} \mid QH \rangle = \frac{1}{1 - n_{f\sigma}^0} \langle 0 \mid \hat{c}_{k\sigma}^+ \hat{f}_{\sigma} \mid 0 \rangle S_6(\sigma)$$

$$\langle LHB \mid \hat{H}_{local} \mid LHB \rangle = S_7(\sigma)$$

$$\langle LHB \mid \hat{H}_{local} \mid QH \rangle = \frac{\sqrt{n_{f\sigma}^0}}{\sqrt{1 - n_{f\sigma}^0}} S_5(\sigma)$$

$$\langle QH|\hat{H}_{local}|QH\rangle = \frac{n_{f\sigma}^0}{1-n_{f\sigma}^0}S_6(\sigma)$$

### 3. $H_V$

$$\begin{aligned} \langle +k_1\sigma|\hat{H}_V|+k_2\sigma\rangle &= \sum_{k'\sigma'} V_{k'\sigma'}[\delta_{\sigma\sigma'}z_\sigma(\langle 0|\hat{c}_{k_1\sigma}\hat{c}_{k'\sigma}^+\hat{f}_\sigma\hat{c}_{k_2\sigma}^+|0\rangle + \langle 0|\hat{c}_{k_1\sigma}\hat{f}_\sigma^\dagger\hat{c}_{k'\sigma}\hat{c}_{k_2\sigma}^+|0\rangle) \\ &\quad + (1-\delta_{\sigma\sigma'}) (\langle 0|\hat{c}_{k'\sigma}^+\hat{f}_{\sigma'}|0\rangle + \langle 0|\hat{f}_{\sigma'}^\dagger\hat{c}_{k'\sigma'}|0\rangle) \\ &\quad \times (x_{\sigma\sigma'}\langle 0|\hat{c}_{k_1\sigma}\hat{c}_{k_2\sigma}^+\hat{f}_\sigma^\dagger\hat{f}_\sigma|0\rangle + v_{\sigma\sigma'}\langle 0|\hat{c}_{k_1\sigma}\hat{c}_{k_2\sigma}^+\hat{f}_\sigma\hat{f}_\sigma^\dagger|0\rangle)] \end{aligned}$$

$$\begin{aligned} \langle +k\sigma|\hat{H}_V|UHB\rangle &= \sum_{k'\sigma'} V_{k'\sigma'}[\delta_{\sigma\sigma'}\langle 0|\hat{c}_{k\sigma}\hat{c}_{k'\sigma}^+\hat{f}_\sigma\hat{f}_\sigma^\dagger|0\rangle \\ &\quad + (1-\delta_{\sigma\sigma'})\langle 0|\hat{c}_{k\sigma}\hat{f}_\sigma^\dagger|0\rangle (y_{\sigma\sigma'}\langle 0|\hat{c}_{k'\sigma}^+\hat{f}_{\sigma'}|0\rangle + w_{\sigma\sigma'}\langle 0|\hat{f}_{\sigma'}^\dagger\hat{c}_{k'\sigma'}|0\rangle)] \end{aligned}$$

$$\begin{aligned} \langle +k\sigma|\hat{H}_V|QE\rangle &= \sum_{k'\sigma'} V_{k'\sigma'}[\delta_{\sigma\sigma'}z_\sigma\langle 0|\hat{c}_{k\sigma}\hat{c}_{k'\sigma}^+\hat{f}_\sigma\hat{f}_\sigma^\dagger|0\rangle \\ &\quad + (1-\delta_{\sigma\sigma'})x_{\sigma\sigma'}\langle 0|\hat{c}_{k\sigma}\hat{f}_\sigma^\dagger|0\rangle (\langle 0|\hat{c}_{k'\sigma}^+\hat{f}_{\sigma'}|0\rangle + \langle 0|\hat{f}_{\sigma'}^\dagger\hat{c}_{k'\sigma'}|0\rangle)] \end{aligned}$$

$$\langle UHB|\hat{H}_V|UHB\rangle = \sum_{k'\sigma'} V_{k'\sigma'}(1-\delta_{\sigma\sigma'})v_{\sigma\sigma'}(1-n_{f\sigma}^0)(\langle 0|\hat{c}_{k'\sigma}^+\hat{f}_{\sigma'}|0\rangle + \langle 0|\hat{f}_{\sigma'}^\dagger\hat{c}_{k'\sigma'}|0\rangle)$$

$$\langle UHB|\hat{H}_V|QE\rangle = \sum_{k'\sigma'} V_{k'\sigma'}(1-\delta_{\sigma\sigma'})(1-n_{f\sigma}^0)(w_{\sigma\sigma'}\langle 0|\hat{c}_{k'\sigma}^+\hat{f}_{\sigma'}|0\rangle + y_{\sigma\sigma'}\langle 0|\hat{f}_{\sigma'}^\dagger\hat{c}_{k'\sigma'}|0\rangle)$$

$$\langle QE|\hat{H}_V|QE\rangle = \sum_{k'\sigma'} V_{k'\sigma'}(1-\delta_{\sigma\sigma'})x_{\sigma\sigma'}(1-n_{f\sigma}^0)(\langle 0|\hat{c}_{k'\sigma}^+\hat{f}_{\sigma'}|0\rangle + \langle 0|\hat{f}_{\sigma'}^\dagger\hat{c}_{k'\sigma'}|0\rangle)$$



$$\begin{aligned}
\langle -k_1\sigma | \hat{H}_V | -k_2\sigma \rangle &= \sum_{k'\sigma'} V_{k'\sigma'} [\delta_{\sigma\sigma'} z_\sigma (\langle 0 | \hat{c}_{k_1\sigma}^+ \hat{c}_{k'\sigma}^+ \hat{f}_\sigma \hat{c}_{k_2\sigma} | 0 \rangle + \langle 0 | \hat{c}_{k_1\sigma}^+ \hat{f}_\sigma^\dagger \hat{c}_{k'\sigma} \hat{c}_{k_2\sigma} | 0 \rangle) \\
&\quad + (1 - \delta_{\sigma\sigma'}) (\langle 0 | \hat{c}_{k'\sigma'}^+ \hat{f}_{\sigma'} | 0 \rangle + \langle 0 | \hat{f}_{\sigma'}^\dagger \hat{c}_{k'\sigma'} | 0 \rangle) \\
&\quad (x_{\sigma\sigma'} \langle 0 | \hat{c}_{k_1\sigma}^+ \hat{c}_{k_2\sigma} \hat{f}_\sigma^\dagger \hat{f}_\sigma | 0 \rangle + v_{\sigma\sigma'} \langle 0 | \hat{c}_{k_1\sigma}^+ \hat{c}_{k_2\sigma} \hat{f}_\sigma \hat{f}_\sigma^\dagger | 0 \rangle)]
\end{aligned}$$

$$\begin{aligned}
\langle -k\sigma | \hat{H}_V | LHB \rangle &= \sum_{k'\sigma'} V_{k'\sigma'} [\delta_{\sigma\sigma'} \langle 0 | \hat{c}_{k\sigma}^+ \hat{f}_\sigma^\dagger \hat{c}_{k'\sigma} \hat{f}_\sigma | 0 \rangle \\
&\quad + (1 - \delta_{\sigma\sigma'}) \langle 0 | \hat{c}_{k\sigma}^+ \hat{f}_\sigma | 0 \rangle (w_{\sigma\sigma'} \langle 0 | \hat{c}_{k'\sigma'}^+ \hat{f}_{\sigma'} | 0 \rangle + y_{\sigma\sigma'} \langle 0 | \hat{f}_{\sigma'}^\dagger \hat{c}_{k'\sigma'} | 0 \rangle)]
\end{aligned}$$

$$\begin{aligned}
\langle -k\sigma | H_V | QH \rangle &= \sum_{k'\sigma'} V_{k'\sigma'} [\delta_{\sigma\sigma'} z_\sigma \langle 0 | c_{k\sigma}^+ f_\sigma^\dagger c_{k'\sigma} f_\sigma | 0 \rangle \\
&\quad + (1 - \delta_{\sigma\sigma'}) v_{\sigma\sigma'} \langle 0 | c_{k\sigma}^+ f_\sigma | 0 \rangle (\langle 0 | c_{k'\sigma'}^+ f_{\sigma'} | 0 \rangle + \langle 0 | f_{\sigma'}^\dagger c_{k'\sigma'} | 0 \rangle)]
\end{aligned}$$

$$\langle LHB | \hat{H}_V | LHB \rangle = \sum_{k'\sigma'} V_{k'\sigma'} (1 - \delta_{\sigma\sigma'}) x_{\sigma\sigma'} n_{f\sigma}^0 (\langle 0 | \hat{c}_{k'\sigma'}^+ \hat{f}_{\sigma'} | 0 \rangle + \langle 0 | \hat{f}_{\sigma'}^\dagger \hat{c}_{k'\sigma'} | 0 \rangle)$$

$$\langle LHB | H_V | QH \rangle = \sum_{k'\sigma'} V_{k'\sigma'} (1 - \delta_{\sigma\sigma'}) n_{f\sigma}^0 (y_{\sigma\sigma'} \langle 0 | c_{k'\sigma'}^+ f_{\sigma'} | 0 \rangle + w_{\sigma\sigma'} \langle 0 | f_{\sigma'}^\dagger c_{k'\sigma'} | 0 \rangle)$$

$$\langle QH | H_V | QH \rangle = \sum_{k'\sigma'} V_{k'\sigma'} (1 - \delta_{\sigma\sigma'}) v_{\sigma\sigma'} n_{f\sigma}^0 (\langle 0 | c_{k'\sigma'}^+ f_{\sigma'} | 0 \rangle + \langle 0 | f_{\sigma'}^\dagger c_{k'\sigma'} | 0 \rangle)$$

---

[1] Hohenberg P and Kohn W 1964 *Phys. Rev.* **136** B864.

Kohn W and Sham L J 1965 *Phys. Rev.* **140** A1133.

[2] Anisimov V I, Zaanen J and Andersen O K 1991 *Phys. Rev. B* **44** 943.

[3] Anisimov V I, Aryasetiawan F and Lichtensten A I 1997 *J.Phys.: Condens. Matter* **9** 767.

[4] Mott, N. F., 1949, *Proc. Phys. Soc. A* **62**, 416.

[5] Mott, N. F., 1956, *Can. J. Phys.* **34**, 1356.

- [6] Mott, N. F., 1961, *Philos. Mag.* **6**, 287.
- [7] Gutzwiller, M. C., 1965, *Phys. Rev.* **137**, A1726.
- [8] Dieter Vollhardt, *Rev. Mod. Phys.* Vol. 56, No. 1, January 1984.
- [9] J. Bünemann, W. Weber and F. Gebhard, *Physical Review B*, **57**, 12 (1998).
- [10] Xiaoyu Deng, Xi Dai and Zhong Fang, *EPL*, **83** (2008) 37008.
- [11] Xiaoyu Deng et al, unpublished.
- [12] Georges A, Kotliar G, Krauth W and Rozenberg M J, 1996 *Rev. Mod. Phys.* **68** 13.
- [13] Mott, N. F., 1990, *Metal Insulator Transitions* (Taylor and Francis, London.)
- [14] Tsuda, N., K. Nasu, A. Yanase, and K. Siratori, 1991, *Electronic Conduction in Oxides*, Springer Series in Solid State Sciences Vol. 94 (Springer-Verlag, Berlin).
- [15] M. Jarrell, Th. Maier, M. H. Hettler and A. N. Tahvildarzadeh, *Phys. Rev. Lett.* **98**, 016402 (2007).
- [16] Qimiao Si, Silvio Rabello, Kevin Ingersent and J. Llewellyn Smith, *Nature* **413**, 804 - 808 (25 Oct 2001).
- [17] Philipp Gegenwart, Qimiao Si and Frank Steglich, arXiv:0712.2045v2.
- [18] V I Anisimov, A I Poteryaev, M A Korotin, A O Anokhin and G Kotliar 1997 *J.Phys.: Condens. Matter* **9** 7359.
- [19] Dai. X, S. Y. Savrasov, G. Kotliar, A. Migliori, H. Ledbetter, and E. Abrahams, 2003, *Science* **300**, 953.
- [20] J. H. Shim, K. Haule, G. Kotliar, 1 November 2007/ Page 3/10.1126/science.1149064.
- [21] G. Kotliar, S. Y. Savrasov, K. Haule, V. S. Oudovenko, O. Parcollet and C. A. Marianetti, *Rev. Mod. Phys.* **78** 865 (2006).
- [22] K. Held, eprint: cond-mat/0511293 unpublished.
- [23] H. O. Jeschke and G. Kotliar *Phys. Rev. B* **71**, 085103(2005).
- [24] S. Y. Savrasov, V. Oudovenko, K. Haule, D. Villani, G. Kotliar, arXiv:cond-mat/0410410v1.
- [25] M.J. Han, X. Wan, S.Y. Savrasov, arXiv:0806.0408v1.
- [26] M. J. Rozenberg, G. Kotliar, and X. Y. Zhang, *Phys. Rev. B* **49**, 10181(1994).
- [27] S. Y. Savrasov, V. Oudovenko, K. Haule, D. Villani, and G. Kotliar *Phys. Rev. B* **71**, 115117(2005).
- [28] M. Jarrell, and Th. Pruschke, *Phys. Rev. B* **49**, 1458 (1994); K. Haule, V. Oudovenko, S. Y. Savrasov, and G. Kotliar, *Phys. Rev. Lett.* **94**, 036401 (2005).

- [29] L. Chioncel, L. Vitos, I. A. Abrikosov, J. Kollr, M. I. Katsnelson, and A. I. Lichtenstein, Phys. Rev. B **67**, 235106(2003); V. Drchal, V. Janiš, J. Kudrnovsk, V. S. Oudovenko, X. Dai, K. Haule, and G. Kotliar, J. Phys.: Cond. Matt. **17**, 61 (2005).
- [30] Michel Caffarel and Werner Krauth, Physical Review Letters **72**, 10.
- [31] L. Laloux, A. Georges, and W. Krauth, Phys. Rev. B **50**, 3092(1994).
- [32] Hirsch, J. E., and R. M. Fye, 1986, Phys. Rev. Lett. **56**, 2521.
- [33] R. Bulla, A. C. Hewson and Th. Pruschke, J. Phys.: Condens. Matter **10** (1998) 8365-8380.
- [34] P. Werner, A. Comanac, L. de' Medici, M. Troyer, and A. J. Millis, Physical Review Letter **97**, 076405 (2006).
- [35] A. N. Rubtsov, V. V. Savkin, and A. I. Lichtenstein<sup>3</sup>, PRB, **72** 035122(2005).
- [36] X. Dai, S. Y. Savrasov, G. Kotliar, A. Migliori, H. Ledbetter, and E. Abrahams, Science 9 May 2003 **300**: 953-955.
- [37] K. Haule, J. H. Shim and G. Kotliar, Phys. Rev. Lett. **100**, 226402 (2008).
- [38] T. M. Rice & K. Ueda, Phys. Rev. B **34**, 9 (1986).
- [39] Shiba, H. & Fazekas, P. (1990). *Prog. Theor. Phys. Suppl.* **101**, 403.
- [40] Fei Tan, Qiang-Hua Wang, Phys. Rev. Lett. **100**, 117004 (2008).
- [41] X. Dai , G. Kotliar and Z. Fang eprint : cond-mat/0611075.
- [42] A. L. Fetter and J. D. Walecka, *Quantum Theory of Many-Particle Systems* (McGraw-Hill, New York, 1971).
- [43] O. Gunnarsson and K. Schönhammer, Phys. Rev. B **28**, 8 (1983).
- [44] A. C. Hewson, *The Kondo Problem to Heavy Fermions*, Cambridge university press
- [45] S. Sugano, Y. Tanabe, and H. Kamimura, *Multiplets of Transition-Metal Ions in Crystals*, Pure and Applied Physics Vol.33 (Academic New York, 1970).
- [46] Kensuke Inaba and Akihisa Koga, arXiv:cond-mat/0603470v1.
- [47] A. Koga, N. Kawakami, T. M. Rice, and M. Sigrist, Phys. Rev. Lett. **92**, 216402 (2004).
- [48] L. de' Medici, A. Georges, S. Biermann, Phys. Rev. B **72**, 205124 (2005)

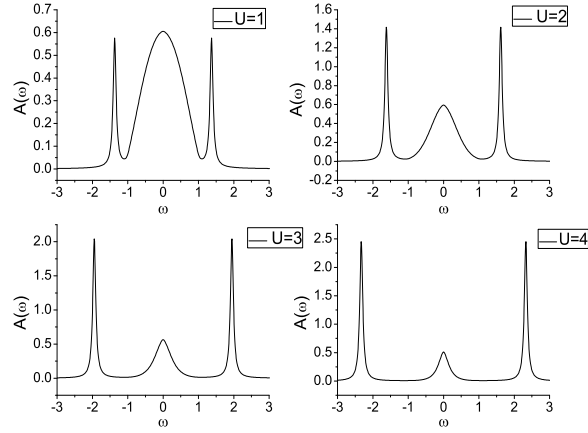


FIG. 1: The spectral function of electrons on the impurity site for an single orbital impurity model with different  $U$  and semi-circular density of states in the bath.

FIG. 2: The spectral function of electrons on the impurity site for an single orbital impurity model obtained by TMA and GA lattice with  $U = 1$ .

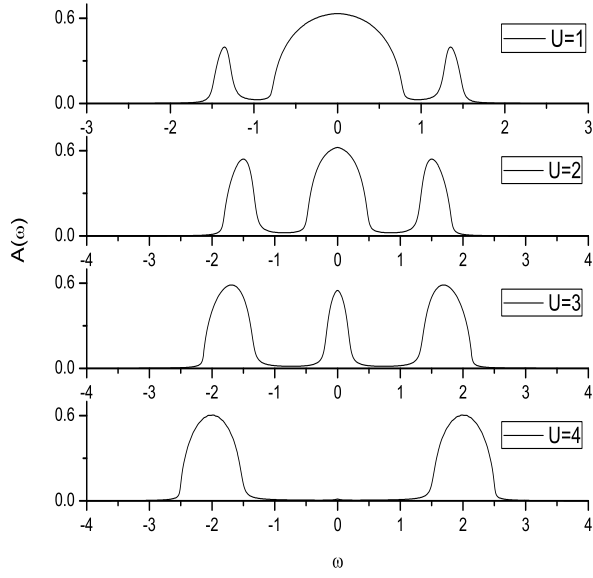


FIG. 3: The density of states (DOS) obtained by DMFT+TMA for single-band Hubbard model on Bethe lattice at half filling.

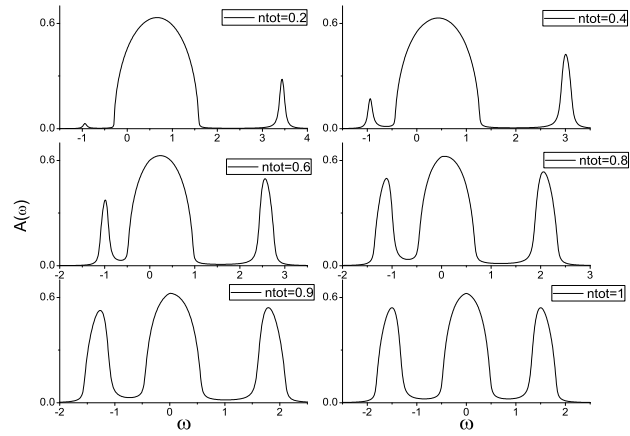


FIG. 4: The density of states (DOS) obtained by DMFT+TMA of single band Hubbard model under  $U = 2$  with different fillings.

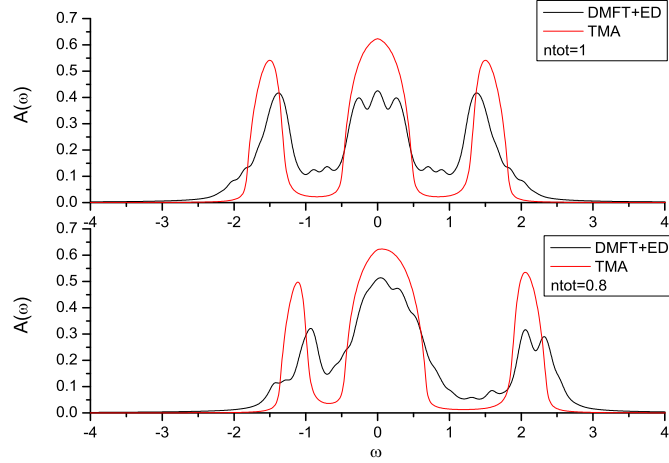


FIG. 5: Comparison of the DOS obtained by DMFT+TMA and DMFT+ED for single band Hubbard model with  $U = 2$ .

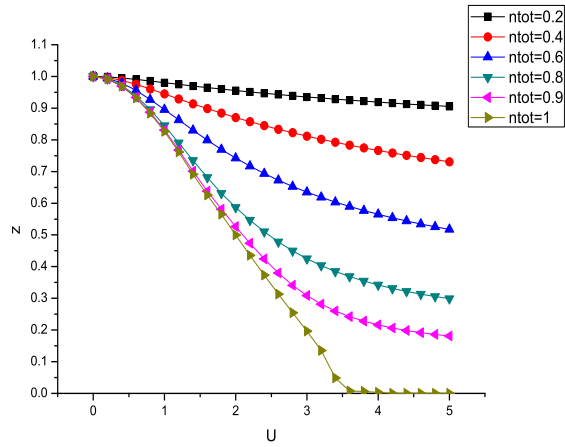


FIG. 6: Quasi-particle weight  $z$  of single band Hubbard model obtained by DMFT+TMA versus  $U$  at different fillings.

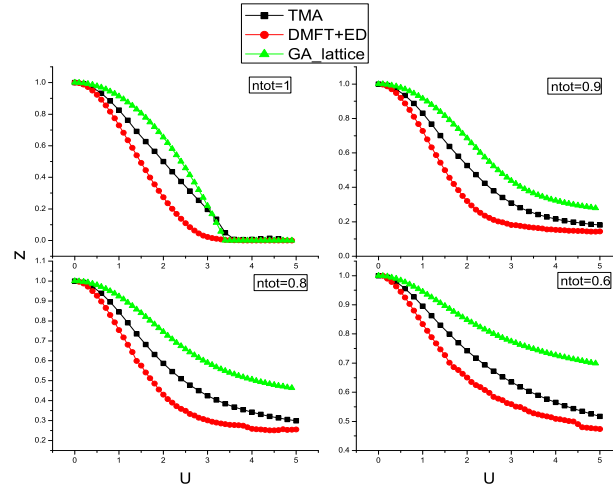


FIG. 7: Comparison of Quasi-particle weight  $z$  for the single band Hubbard model obtained by DMFT+TMA, GA lattice and DMFT+ED.

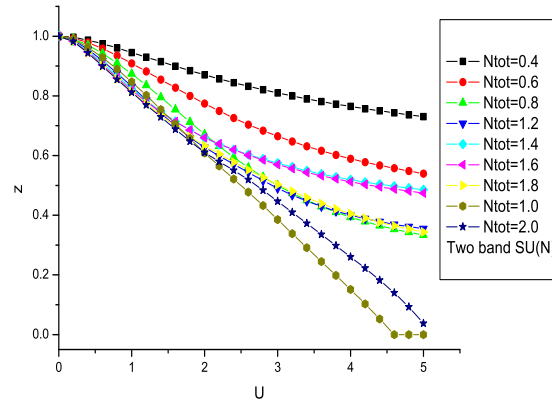


FIG. 8: Quasi-particle weight  $z$  as the function of  $U$  for the two-band Hubbard model with  $SU(N)$  symmetry obtained by DMFT+TMA.

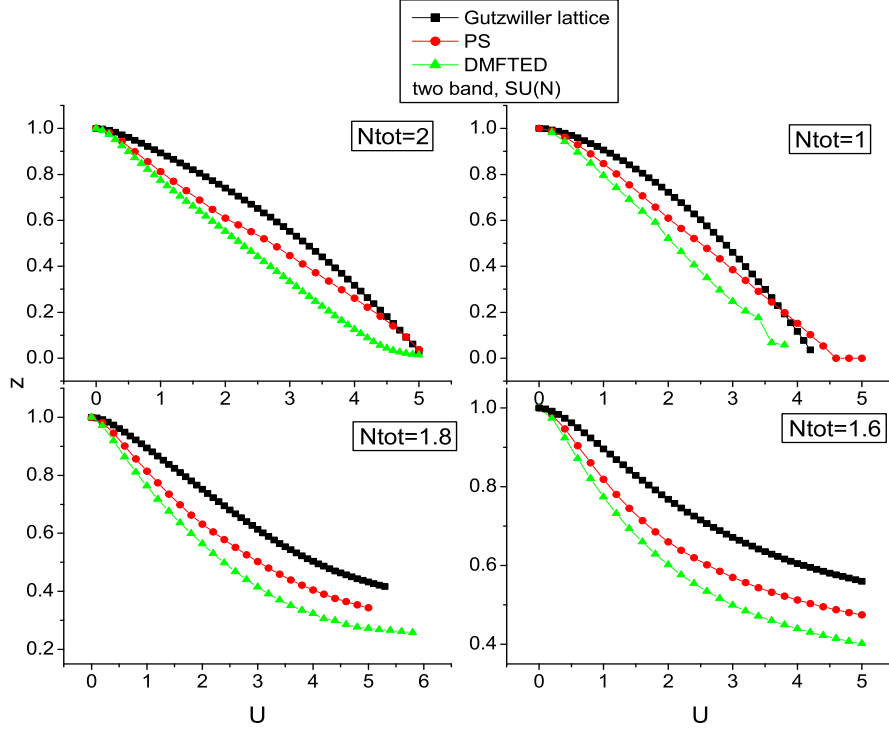


FIG. 9: Comparison of quasi-particle weight  $z$  for the two band Hubbard model with  $SU(N)$  symmetry at different fillings obtained by DMFT+TMA, GA lattice and DMFT+ED.

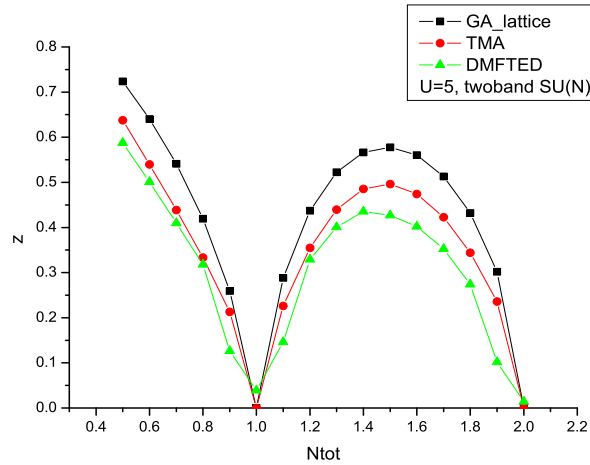


FIG. 10: Comparison of quasi-particle weight  $z$  as the function of total number of particles for the two-band Hubbard model with  $SU(N)$  symmetry at  $U = 5$  obtained by DMFT+TMA, GA lattice and DMFT+ED.



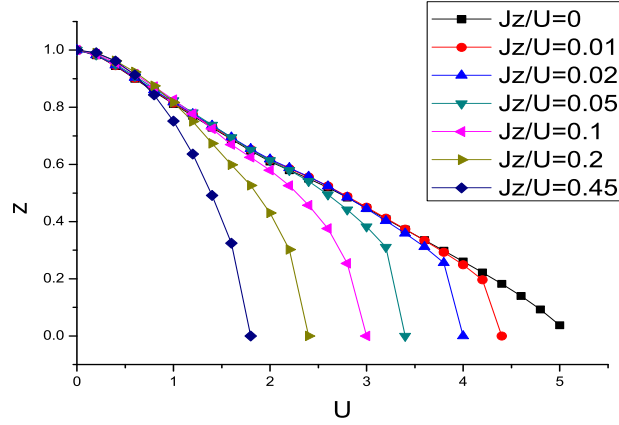


FIG. 11: Quasi-particle weight  $z$  as the function of  $U$  for the two-degenerate-band Hubbard model with longitudinal Hund's coupling  $J_z$  obtained by DMFT+TMA at different  $J_z/U$ .

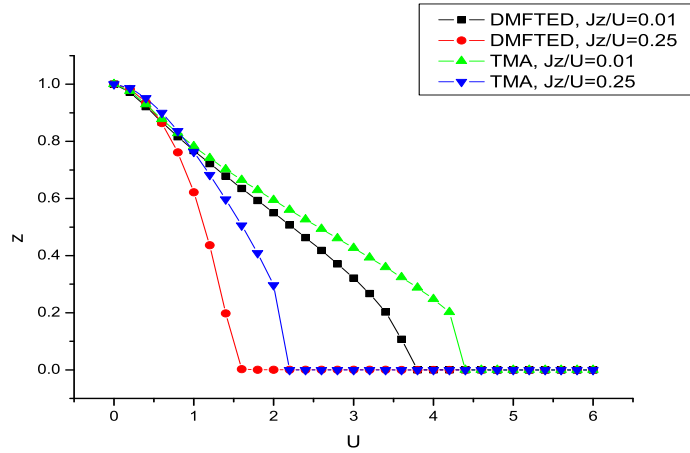


FIG. 12: Comparison of quasi-particle weight  $z$  for the two-degenerate-band Hubbard model with longitudinal Hund's coupling  $J_z$  obtained by DMFT+TMA and DMFT+ED at different  $J_z/U$ .

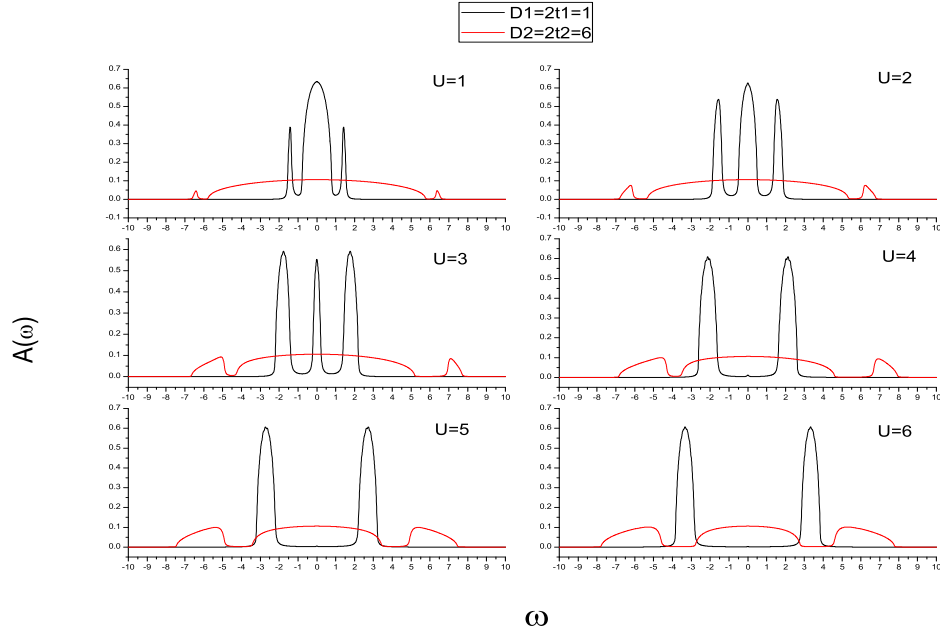


FIG. 13: The spectral functions obtained by DMFT+TMA for two-nondegenerate-band Hubbard model with band width ratio 1 : 6 under different  $U$  with  $J_z = 0.3U$ .

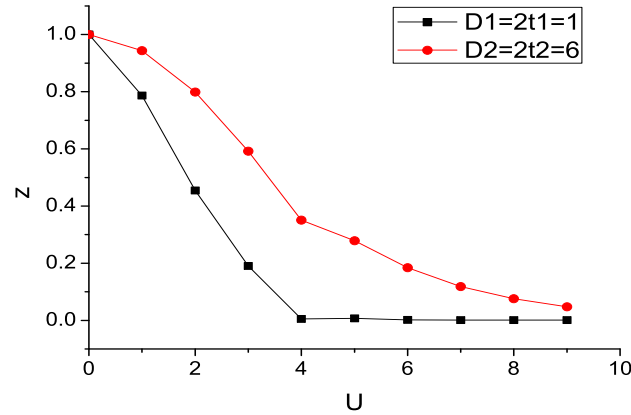


FIG. 14: Quasi-particle weight  $z$  of different bands as the function of  $U$  for two-nondegenerate-band Hubbard model with band width ratio 1 : 6 under different  $U$  with  $J_z = 0.3U$ .

